UNIVERSITY OF TURKISH AERONAUTICAL ASSOCIATION
INSTITUTE OF SCIENCE AND TECHNOLOGY

EXPERIMENTAL STUDY OF SHELL AND TUBE HEAT EXCHANGER PERFORMANCE USING AL_2O_3\WATER AND TIO_2\WATER NANOFLUIDS

Master Thesis

Raed Khalid ABDULLAH

1406080020

IN PARTIAL FULFILLMENT OF THE REQUIREMENT FOR THE DEGREE OF MASTER OF SCIENCE IN MECHANICAL AND AERONAUTICAL ENGINEERING

Thesis Supervisor: Assist. Prof. Dr. Mohamed ELMNEFI

Raed Khalid ABDULLAH M.R, having student number 1406080020 and enrolled in the Master Program at the Institute of Science and Technology at the University of Turkish Aeronautical Association, after meeting all of the required conditions contained in the related regulations, has successfully accomplished, in front of the jury, the presentation of the thesis prepared with the title of: **Experimental Study of Shell and Tube Heat exchanger Performance using Al_2O_3\water and TiO_2\water Nanofluids.**

Supervisor : **Assist. Prof. Dr. Mohamed Salem Elmnefi**
University of Turkish Aeronautical Association .....

Jury Members : **Assoc. Prof. Dr. Mecit YAMAN**
University of Turkish Aeronautical Association .....

: **Assist. Prof. Dr. Mohamed Salem Elmnefi**
University of Turkish Aeronautical Association .....

: **Assist. Prof. Dr. Munir ELFARRA**
Yildirim Beyazit University- Ankara .....

Thesis Defense Date: 21.12.2017

STATEMENT OF NON-PLAGIARISM PAGE

I hereby declare that all the information in this study I presented as my Master's Thesis, called "Experimental Study of Shell and Tube Heat exchanger Performance using Al_2O_3\water and TiO_2\water Nanofluids." has been presented in accordance with the academic rules and ethical conduct. I also declare and certify on my honor that I have fully cited and referenced all the sources I made use of in this present study.

Raed ABDULLAH M.R.

Date 21/12/2017

ACKNOWLEDGEMENTS

. I am grateful to The Almighty ALLAH for helping me to complete this thesis. My Lord mercy and peace be upon our leader “Prophet Mohammed” peace is upon on him, who invites us to science and wisdom, and members of his family and his followers.

I would like to express my deep gratitude for my supervisor, Dr. Mohamed Salem Elmnefi, I will forever be beholden to his sincere support and encouragement. His extreme generosity will be remembered in all my life. It is so hard to find words to express my gratitude for his supervision and devotion.

My parents, I missed you so much, and I wished that you are beside me now more than any times and more than anyone else. I would like to pay my life to see your faces again, to kiss your blessed hands. There are no happiness, no ambitious and no hope without you. My beloved father, I have achieved what you want me to achieve, But with a lot of grief, without you.

Last, but not least, I would like to thank my wife for her patience, supporting and encouragement, to my invaluable sons (Bahjat, Khalid) and my beautiful daughters (Raghad, Farah). Thanks to my brothers (Ayad, Ahmed, Mahmood, Anas and Suhaib), my uncle and my aunt (Ibrahim, Jazya) and my sisters who always pray for me to get success. To all my friends and all who gave a hand, I say thank you very much.

December 2017 Raed Khalid ABDULLAH M.R.

TABLE OF CONTENTS

LIST OF TABLES

LIST OF FIGURES

NOMENCLATURE

Cp	Specific heat, J/kg K
d	Tube diameter, m
h	Overall heat transfer coefficient, W/m^2 K
ΔT_m	Logarithmic mean temperature difference °C
K	Conductivity, W/m.K
m°	Mass flow rate, L/m
V°	Volume flow rate
Nu	Nusselt number
Re	Reynolds number
Pr	Prandtl number
Q	Heat transfer, W
T	Temperature, °C
V	Mean velocity, m/s
F	Correction factor
As	Surface area
Ac	Cross section area
L	Length

GREEK SYMBOLS

υ	Kinematic viscosity, m^2/s
μ	Dynamic viscosity (kg/m.s)
∅	Volume concentration, %
ρ	Density, kg/m^3
σ	Standard deviation

SUBSCRIPTS

in	Inlet
out	Outlet
nf	Nanofluid
b	Base fluid
n.p.	Nanoparticles
m	Mean
h	Hot
c	Cold

ABSTRACT

EXPERIMENTAL STUDY OF SHELL AND TUBE HEAT EXCHANGER PERFORMANCE USING AL_2O_3\WATER AND TIO_2\WATER NANOFLUIDS

ABDULLAH, Raed

M.Sc., Department of Mechanical Engineering

Supervisor: Assist. Prof. Dr. Mohamed Salem Elmnefi

December 2017, 83 pages

There are various enhancement-techniques may lead to a significant reduction in energy consumption and increasing the efficiency of power plants. The compact heat exchangers, Shell & Tube is an important part in power plants cooling system, it is one of the widely type of heat exchangers which is used in this region in which water or water mixed with ethylene glycol are used as conventional coolants. It is very important to find new effective and convenient approaches to enhance the efficiency of shell and tube heat exchanger. One of the approaches is replacing water with a higher thermal conductivity fluid containing solid nanoparticles known as Nanofluid.

In this study, the effect of utilizing (TiO_2\water and Al_2O_3\water) nanofluids as well as water in shell and tube heat exchanger was presented and discussed. The experimental results of water and these nanofluids evaluated based on the effect of varying volume concentrations of 0.1, 0.2 and 0.3% of each kind of nanofluids in turbulent flow rates of 5, 5.5, 6, 6.5 and 7 L/m for each concentration of the proposed nanofluids and water on the activity of the heat exchanger. The parameters of heat transfer rate, heat transfer coefficient hi, over all heat transfer coefficient, Reynolds number and Nusselt number were calculated according to the equations that were related with these situations, and the results of all experiments were analyzed to create a comparison among them.

The results revealed that heat transfer rate, heat transfer coefficient, over all heat transfer coefficient and Reynolds number increased with increasing of the volume concentration of the nanofluid. In addition, they are higher in Al_2O_3\water than TiO_2\water and water, respectively. The highest value of heat transfer rate, heat transfer coefficient, over all heat transfer coefficient and Reynolds number are 1741.54(W), 4414.96(W\m.c), 1326.86(W\m^2.c) and 4425.86 in Al_2O_3\water

nanofluid in concentration of 0.3% and flow rate of 7L\m, respectively. The highest value of Nusselt number is 34.37 in TiO_2\water nanofluid in concentration of 0.3% and flow rate of 7L\m.

Keywords: Shell and tube heat exchanger, Heat transfer rate, Base fluid or water, Nanofluid, Nanopowder, Heat exchanger, counter flow heat exchanger.

ÖZET

AL_2O_3\SU VE TIO_2\SU NANOAKIŞLARININ KULLANILDIĞI HUZME BORULU ISI EŞANJÖRLERİN DENEYSEL ÇALIŞMASI

ABDULLAH, Raed

Makine Mühendisliği Bölümü Yüksek Lisansı

Denetçi: Yrd. Doç. Dr. Mohamed Salem Elmnefi

Aralık 2017, 83 sayfa

Bu çeşitli geliştirme teknikleri, enerji tüketiminde kayda değer bir azalmaya ve enerji santrallerinin etkinliğini artırmaya yol açabilir. Kompakt ısı eşanjörleri olan Huzme Borulu, enerji santrallerin soğutma sisteminde önemli bir parça iken; aynı zamanda klasik su soğutma maddesi olarak etilen glikol ile karıştırılmış su ya da suyun kullanıldığı bu bölgede kullanılan yaygın ısı eşanjörlerinden biridir. Huzme Borulu Isı Eşanjörünün verimliliğini artırmak adına etkili ve kullanılabilir yaklaşımlar elde etmek çok önemlidir. Yaklaşımlardan biri, suyun nanoakışkan olarak bilinen katı nano partikül içeren bir daha yüksek termal iletkenlik sıvısı ile yer değiştirmektedir.

Bu çalışmada, huzme borulu ısı eşanjöründeki suyun yanı sıra kullanılan nanoakışkanların(TiO_2\su ve Al_2O_3\su) etkisi ortaya koyulmuş ve tartışılmıştır. Su ve bu nanoakışkanların deneysel sonuçları, önerilen nanoakışkanların her bir konsantrasyonu için 5, 5.5, 6, 6.5 ve 7 L/m türbülanslı akış oranlarında her bir tür nanoakışkanın % 0.1, 0.2 ve 0.3'lik muhtelif hacimdeki konsantrasyonlarının etkisi ve ısı eşanjörünün aktivitesindeki su temelinde değerlendirilmiştir. Isı aktarım oranı, ısı aktarım katsayısı, genel ısı aktarım katsayısı, Reynolds numaralsı ve Nusselt numarası parametreleri, bu durumlarla ilgili olan eşitlikler uyarınca hesaplanmış olup

ve tüm denemelerin sonuçları, bunların arasında bir kıyaslama yaratabilmek amacıyla analiz edilmiştir.

Sonuçlar, ısı aktarım oranı, ısı aktarım katsayısı, genel ısı aktarım katsayısı ve Reynolds numarasının, nanoakışkanının hacimsel konsantrasyonunun artışıyla artmış olduğunu açıklığa kavuşturmaktadır. Ayrıca bunlar, Al_2O_3\'de sırasıyla TiO2\su ve suda olduğundan daha yüksektir. Isı aktarım oranı, ısı aktarım katsayısı, genel ısı aktarım katsayısı ve Reynolds numarasının en yüksek değeri, sırasıyla 1741.54(W), 4414.96(W\m.c), 1326.86(W\m2.c) olup ve % 0.3'lük konsantrasyonda Al2O3\suda 4425.86 ve 7L\m'lik bir akış oranıdır. % 0.3'lük kontrasyonda 7L\m'lik akış oranındaki TiO_2\sudaki en yüksek Nusselt değeri 34.37'dir.

Anahtar Sözcükler: Huzme Borulu Isı Eşanhörü, Isı aktarım oranı, Temel akışkan veya su, Nanoakışkan, Nano toz, Isı eşanjörü, ters akışlı ısı eşanjörü.

CHAPTER ONE

INTRODUCTION

1.1 Motivation

Nowadays, there is a great potential toward optimizing the energy consumption in industry due to increasing world demands for energy, the high cost of energy, and the associated environmental pollution with the fossil fuels and their limitations [1]. Heat transfer units such as heat exchangers are playing an important role in various industrial applications (chemical and petrochemical engineering, oil and gas refinery, air-conditioning automotive industry, and many other applications) [1]. In order to meet the above energy requirements, there is a numerous interest in improving efficiency of the heat exchanger. Among different kinds of heat exchanger, shell and tube counter flow heat exchanger is one of the most used units in several industrial processes. However, there is still a need for enhancing its efficiency. One of the most efficient approach to reach this goal is replacing the base fluid with the nanofluid that contains nanosized particles of metals or metal oxides or organic materials [2]. Engineers are usually being requested to improve processes and increase efficiency of the industrial units. Increasing the process throughout, increasing profitability or accommodate capital barriers may cause rising up these requests. Therefore, transferring thermal energy by heat units with maximum heat transfer rate and low cost is very essential.

1.2 Heat Transfer and Thermodynamics

Heat transfer is the branch of thermal engineering that focuses on prediction the energy transfer that may take place between material bodies because of a temperature difference as shown in Fig. (1.1). Heat transfers by different methods,

which are conduction, convection, radiation, and phase changes[3]. Heat transfer is an important phenomenon in various industrial applications such as chemical and petrochemical processes, oil and natural gas refinery, electronic and electrical devices, space heating, and air-conditioning [1].

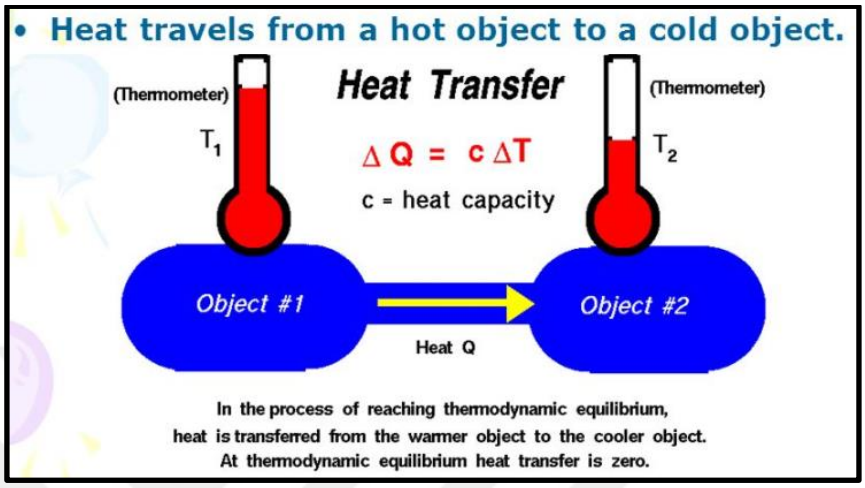

Figure (1.1): Heat transfer due to temperature difference.

Thermodynamics is the branch of physics, which deals with heat and temperature and their relations with other forms of energy. Thermodynamic should be noted that heat tells us how heat is transferred, at what rate, and the temperature distribution inside the body, while thermodynamic provides information on how much heat is transferred, how much work is done, and the final state of the system.

1.3 Shell and Tubes Heat Exchangers

The function of a heat exchanger is to exchange heat between two streams; one contains a hot fluid and another one carries a cold fluid before introducing one of them to the next operation unit. Compared to the other types of heat exchangers, the shell and tube heat exchanger is one of the most traditional used equipment in oil refinery and large chemical and petrochemical factories [1][2],[4],[5]. Figure (1.2) shows schematic of an example of one of several kinds of shell and tube heat exchanger. It consists of a number of tubes incorporated inside a shell (a large pressure vessel). The association of tubes is known as a tube bundle, and it is far assembled by using many styles of tubes: plain, longitudinally finned, etc. Heat

exchangers run on the concept of convective and conductive heat transfer. Conduction takes place as the heat which was transferred from the hot fluid passes out of the pipes wall [3].

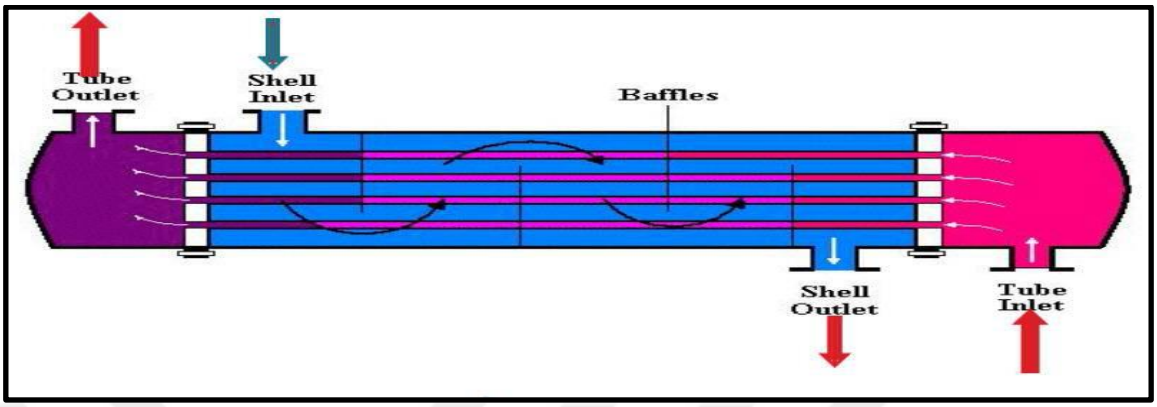

Figure (1.2): Shell and tube heat exchanger.

One fluid flows inside the tubes; another one flows through the shell (over the tubes). Heat is transferred between them by conduction. To increase the heat transfer, the pipe wall has to be skinny and conductive [6]. Various types of heat exchangers are available in industry [7]. Shell and tubes heat exchangers are classified on basis of different parameters like flow rate, compactness of frame transfer type, and production. Based on the flow direction, it can be classified as parallel, counter, and cross flow, as shown in Figure (1.3).

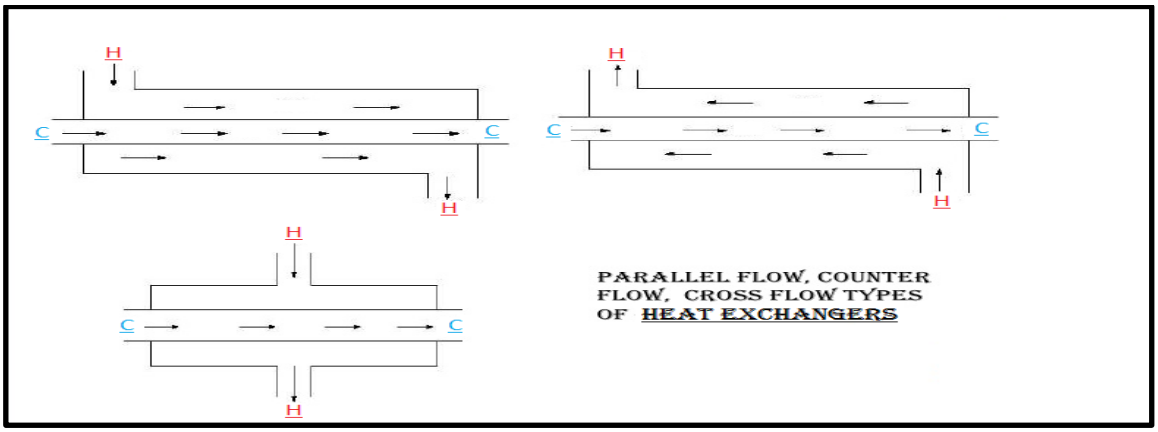

Figure (1.3): Flow patterns of heat exchangers.

Counter flow heat exchanger is an efficient flow technique among other types of flow, as it shown in Figure (4). It leads to the lowest required heat exchanger

surface area due the log mean temperature drop is the highest for counter flow heat exchanger [8].

1.4 Nanofluid Technology and applications

The Nanotechnology defined by National Nanotechnology Initiative (NNI) as the understanding and control of material at dimensions about 1 to 100 nm, where unique phenomena enable new applications. Encompassing nanoscale science, engineering and technology, nanotechnology involves photographing, scaling, modeling, and manipulating matter at this domain. Nanostructured materials can be nanoparticles, nanowires, nanotubes, nanorods, nanoporus materials, and many other structures. In this study, we will focus on the nanoparticles for the nanofluid preparation.

Ten years ago, the fast development of modern nanotechnology, particles of nanometer-size (usually smaller than a hundred nm) were used rather than micrometer-size, for mixing in base liquids [9]. Liquid mixed with nanoparticles known as nanofluid that its thermal conductivity was higher than those which the corresponding base fluids [10]. In general, the nanostructured materials exhibit different and unique properties as compared to the bulk materials with the same compositions. In recent years, several research works executed to comprehend the effect of adding nanoparticles to the base fluids on the efficiency of heat exchangers [11]. Nanoparticles have a high conductivity, and density more than triple value of water density. Therefore, adding nanoparticles to the water increase the density of the new fluid that will called nanofluid. For the same volume flow rate, the mass flow rate of the nanofluid will be more than mass flow rate of the water. This increment in the density leads to enhance the heat transfer rate.

1.5 Thesis objective

Various heat transfer enhancement techniques for improving the performance of heat exchanger systems may guide to a significant decrease in energy consumption. An example of compact heat exchangers, shell and tube is an important part in power plants and engines cooling system in which water or oil or ethylene glycol are used as conventional coolants. For improving the heat transfer rate, it is

very important to find new effective and convenient approaches to enhance the efficiency of shell and tube heat exchanger. One of the approaches is replacing the base fluid (water) with a higher thermal conductivity fluid containing solid nanoparticles known as nanofluid. The characteristics of nanofluid can reduce the size of the shell and tube heat exchanger without affecting its heat transfer performance and resulting in an enhanced power saving. It should be noted that the most of earlier research abstracts were finite to the laminar flow of the coolant apparatus that is not factual and the flow enters into turbulent flow region in these types of cooling systems. Hence, this study will consist on the effect of following parameters on heat transfer rate under turbulent regime: different types of (Al_2O_3) and (TiO_2) of nanoparticles, various concentrations of the nanoparticles and different flow rates of nanofluids.

1.6 Thesis outline

This study includes five chapters to cover the aim of the thesis. Literature review will be included in chapter two to give details and description of the updated studies that focused on the investigation of the performance of shell and tube heat exchanger which using nanofluid. In chapter three, the components of the experimental setup of the heat exchanger as well as the experimental procedure used in this study and they were described in details. The results of the proposed nanofluids flow in shell and tube heat exchanger discussed in chapter four. Finally, conclusion of this work and recommendations for future work are given in chapter five. In this study, water and two types of nanofluids were used in three concentrations of 0.1, 0.2 and 0.3 % for each type of nanofluids in flow rate of 5, 5.5, 6, 6.5 and 7 L/m, for each kind of the fluids.

CHAPTER TWO

LITERATURE REVIEW

In several industrial applications, the nanofluid is considered as a new medium for improving the heat transfer in many heat transfer units such as heat exchangers. Hence, the aim of this chapter is to present up to date literature review regarding utilizing nanofluids in enhancing the heat transfer efficiency of shell and tube heat exchanger. The nanofluid exhibit better thermal properties compared to the base fluids such as water. In this chapter, the literature review will focus on the experimental and numerical research for investigating the performance of the shell and tube heat exchanger using Al_2O_3/ water and TiO_2/water nanofluids. The forced convective heat transfer and flow characteristics of Al_2O_3/water nanofluid in a horizontal, counter flow heat exchanger under turbulent flow regime was investigated experimental. The nanoparticles have a diameter of 30 nm and the nanoparticles volume concentration was varied within the range of (0.3-2%). At the same mass flow rate and inlet temperature, he results indicated that there is a slight enhancement in the heat transfer coefficient of the nanofluid in comparison with water. It was noted that as the mass flow rate and the volume concentration of Al_2O_3 nanoparticle increase, the heat transfer coefficient of the nanofluid increases. However, increasing the concentration of nano powders increased the frication factor due to the enhanced viscosity of the nanofluid [9]. S. Kannan et al. (2014) [5] presented an experimental research for using the nanofluids and their effect on the performance of shell and tube heat exchanger. The authors claimed that adding nanopowders to the base fluid results in enhancing the thermal conductivity and viscosity, leading to the enhanced heat transfer rate. In another study, the convective heat transfer rate of alumina/water nanofluid in shell and tube heat exchanger was investigated experimentally under counter and parallel turbulent flow conditions. The diameter of alumina nanoparticles was about 22 nm and different volume

concentrations (0.13, 0.27, 0.4, and 0.53%) of the nanoparticles were considered for the nanofluid preparation. The author concluded the following: (1) the counter flow shows higher heat transfer rate than that of the parallel flow, (2) the heat transfer rate increases when volume concentration of the nanoparticles increases, and (3) compared to water, the nanofluid doubled the heat transfer rate [11]. R. Dharun Arvind (2015) [10] developed a new nanofluid based on aluminum nitride nanoparticles that mixed with water and the resulting nanofluid was applied as a working fluid in shell and tube heat exchanger. The aluminum nitride was proposed due to its low density, high melting point, and good structural stability. The thermal conductivity and heat transfer coefficient of aluminum nitride/water nanofluid were characterized. The results demonstrated that the proposed nanofluid offers higher thermal conductivity and heat transfer coefficient than those of water; the effectiveness enhancement was about 9.68%. The effects of Peclet number and the nanoparticles volume concentration of Al_2O_3/water nanofluid on the heat transfer and pumping power in shell and tube heat exchanger with the presence a wire coil insert was studied experimentally. Compared to water, the nanofluid offers a significant enhancement in overall heat transfer coefficient as the volume concentration of nano powders the base fluid increases. The combination of the nanofluid and wire coil insert has a positive influence on the heat transfer performance, leading to a higher heat transfer coefficient compared to the base fluid at the same Peclet number. The results demonstrated that at the volume concentrations of 0.5%, 1.0%, and 1.5% of the Al_2O_3 nanoparticles for wire coil insert at Pe = 3000, the overall heat transfer coefficient increased by 17%, 29.4%, and 33.5%, respectively, as compared to the (BF). Compared to the base fluid, the pumping power for the wire coil inset increases significantly by about 13% [12]. K. Karimullah Khan & G. Praveen Kumar Yadav 2016 [13] carried out in them experimental study of using Al_2O_3/water (NF) to enhance heat transfer in a shell and tube heat exchanger for parallel flow heat exchanger and counter flow heat exchanger arrangement. The volume concentrations of Al_2O_3 (NP) were 0.05% and 0.1%. The evaluation of the results was drawn based on the heat transfer rate, shell side and tube side heat transfer coefficient, over all heat transfer coefficient and effectiveness. It is declared that increasing the concentration of nano powders in the nanofluid up to certain stage, leads to an increase in overall heat transfer coefficient. The authors concluded that in addition to the thermal conductivity enhancement, the random movements, dispersions, and

fluctuations of nano powders especially near the tube wall increase the heat exchange rates between the fluid and the tube wall. Ramesh R and R.Vivekananthan 2014 [14] reported the same findings. In this study, at different Reynolds number and 0.2% nano powders volume concentration, Nusselt number increases by 30% in comparison with the base fluid. S. Bhanuteja and D. Azad (2013) [15] studied numerically the thermal performance of various types of (Ag, Al_2O_3, TiO_2, CuO, and SiO_2) nanofluid in counter flow heat exchanger. The three-dimensional steady, turbulent developing flow, and conjugate heat transfer in shell and tube heat exchanger were solved using Finite volume method. The results of these nanofluids used were compared with the base fluid (water). Temperature profiles, heat transfer coefficient, pressure profile, were got from the simulations. The results were evaluated in terms of effectiveness, heat transfer rate, and overall heat transfer coefficient. The conclusion drawn by the authors were not clear enough to decide which nanofluid demonstrates the highest performance based on the above criteria considered by the authors. In another attempt [16], the thermal performance of shell and tube heat exchanger using nanofluids was evaluated mathematically. The nanofluid flows in the tube side and the hot fluid flows inside the shell. The study, demonstrated that as the volume concentration of the nanoparticles increases from 0.5% to 3%, the effectiveness increased by 6.2% with a small due to the application of Al_2O_3/water nanofluid. Moreover, the authors concluded that the nanofluid required less coolant pumping power compared to the water.

Different laminar flow patterns (parallel, counter, and shell and tube) in shell and tube heat exchanger were considered in studying the forced convective heat transfer and flow characteristics of nanofluid consisting of water and 1% volume concentration of Al_2O_3. The diameter of Al_2O_3 nanoparticles was about 50 nm. The experiments were conducted by changing mass flow rates; three mass flow rates were selected. In general, at the same flow rate and inlet temperature, the author concluded that the heat transfer coefficient and dimensionless Nusselt number of nanofluid is slightly higher than that of the base fluid. It was reported that increasing mass flow rate results in an increases in overall heat transfer coefficient of the nanofluid. While, the logarithmic mean temperature difference drops as the Reynolds number increases at 1% nano powders volume concentration. Furthermore, it was concluded that the ratio of overall heat transfer coefficient of Al_2O_3/water nanofluid

to water is 1.161, 1.146, and 1.171 for parallel, counter, and shell and tube heat exchangers, respectively [17]. RAVINDRA M. GHODKE (2017) [18] presented an overview of the most recent development of the application of nanofluids in heat transfer field. Through this review, it is obvious that more attention was paid by researchers to improve the thermophysical properties of the base fluid or the flow and heat characteristics in heat transfer equipment. The authors concluded that the nanofluids have attracted a great interest in enhancing the heat transfer rate for the heat transfer equipment such as heat exchangers and more in depth investigation is required to have better understanding the heat transfer characteristics of nanofluids and discover new and exclusive applications for these fields. However, it should be noted that more effort is also needed to solve the problems associated with the stability of the nanoparticles and the production cost, which are the major obstacles to nanofluids commercialization.

Experimental and numerical study was performed for the sake of investigation the effect of multi-walled carbon nanotubes (MWCNTs)/water nanofluids on the heat transfer coefficients, Nusselt number, friction factor, Euler number and comprehensive thermal performance factor in a helically baffled heat exchanger with elliptic tubes. The results indicated that as the nano powders concentration as well as Reynolds number increases, the convective heat transfer coefficient increases. At the same Reynolds number and the Nusselt number of MWCNTs increase by 11%, 21%, and 35% for 0.2%, 0.5%, and 1.0% weight percent of MWCNTs, respectively. In addition, the comprehensive thermal performance factor factors of the nanofluids are 3-5%, 15-17%, and 24-26% higher than that of water at the same volume flow rate [19]. Ali Heydari et al. (2015) [20] studied the performance of shell and tube heat exchanger with baffles using different nanofluid of (Cu, Fe, Au, Al_2O_3, CuO, and Fe_2O_3) numerically. According to the amount of flow rate, it can enhance the thermos-physical properties that lead to decrease or increase the heat transfer coefficient. In the present study, the effect of different nanofluids with many volume fractions for application in baffled shell and tube heat exchanger was numerically evaluated considering a three-dimensional modeling. At several volume fraction of all (NF), the rate of heat transfer, pressure drop, and outlet shell temperature are estimated. The results declare that the effect of addition of nano particles reduces the heat transfer coefficient, pressure drop, and shell heat transfer

rate but leads to an increase in the outlet shell temperature. An experimental investigation was executed to evaluate the heat transfer characteristics of shell and tube heat exchanger Al_2O_3/water nanofluid with nano powders concentration up to 2 % by volume. At 2 % concentration, the results show an increase in heat transfer rate of 34 %, 44.8 % and 57.6 % for the shell-side flow rate of 2 lpm, 3 lpm, and 4 lpm and tube-side flow rate of 1 lpm, 2 lpm, and 3 lpm, respectively. It was observed that the various energy parameters attained maximum values at concentration of 2 % for different flow rate of fluids at shell and tube side. This upward trend being continued until the viscous force dominates in the flow path. Further rise in heat transfer rate is possible with higher percentage of nanofluid concentration at the cost of pressure drop. This happens if the turbulence is created by adding inserts in the flow path [21]. The flow and heat transfer characteristics of two Al_2O_3 nanoparticles concentration (1% and 2.5% by volume) with particle diameter of 30-60 nm in a straight micro-channels was investigated. The Reynolds numbers were varied from 70 to 300. According to the correlations from the literature, the thermal properties of the nanofluids at the bulk temperature of the fluid were calculated. The results imply that (h) of the 2.5% by volume, Al_2O_3/ water nanofluid enhances by 5.5% compared to distilled water. The improvement increases with Reynolds number. The heat transfer coefficient increases with increasing the volume concentration of the nanofluids. It was found that the velocity measurements show no significant influence on the mass flow rate for Nano fluids [22]. Laith J. Habeeb et al. (2105) [23] presented a review of the numerical and experimental studies for laminar nanofluid flow in a circular tube. The authors concluded the following: (1) there is no a significant effect of increasing the nanoparticles concentration in the range of 0.25% on the heat transfer enhancement, (2) by increasing the (Re), the rate of (h) enhancement of nanofluid to that of pure water decreased, (3) increasing the volume fraction of nanoparticles leads to an increase in the pressure drop, (4) the heat transfer coefficient of the nanofluid is higher than that of water, (5) an increase in the Peclet number and the nanoparticle concentration results in an increase in (h), (6) the thermal conductivity enhancement is much smaller than the effect of the convective heat transfer enhancement of nanofluids, and (7) the local heat transfer coefficient of nanofluid increases with increasing nanoparticle concentration at a certain Peclet number and axial position.

This study is concerned with performing a comparison of two types of nanofluids (Al_2O_3/water and TiO_2/water nanofluid) with the base fluid on heat transfer performance of shell and tube heat exchanger. The Al_2O_3 is one of the most common nanoparticles used in the preparation of the nanofluids for heat transfer applications due to its low cost, availability, and unlike many metal oxide nanoparticles; it is not susceptible to surface oxidation and is much easier to incorporate in the base fluid [24].

Conclusion Remarks

Based on the literature review, it is obvious that generality of the researchers have chosen one specific nanofluid and few studies have suggested two or more specific nanofluids, which enhance the thermal conductivity of the base fluid and this will be reflected positively on heat transfer coefficient in a shell and tube heat exchangers. Hence, more in depth investigation and fair comparison between two or more than two different nanofluids types is required to have better understanding of the role of the nanofluid types, nanoparticle size and volume concentration, and the nanofluid flow rates. On the other hand, it was observed that there are limited studies utilizing TiO_2 nanoparticles in the nanofluid preparation for heat transfer application. Therefore, I proposed carrying out an experimental on different concentrations of this nanofluid to suppose the forced convective heat transfer in shell and tube heat exchanger.

CHAPTER THREE

THE EXPERIMENTAL WORK

The objective of this chapter is to present the experimental setup. The following sections describe the details of the experimental set-up, measuring and auxiliary devices, experimental procedure, and theoretical analysis.

3.1 The Experimental Setup

The schematic diagram of the experimental setup that was used is shown in Figure (3.1), with a photo shows the experimental set-up as demonstrated in Figure (3.2). The experimental setup consists shell and tube heat exchanger, double pipe heat exchanger, two flow loops for cold and hot fluids, and temperature recorder. Each flow loop includes a pump, a flow meter, a reservoir, gate valves to maintain the required flow rate, and other auxiliaries. The cold fluid (water or nanofluid) flows inside the tubes at a constant inlet temperature of (30 ^{o}C), while the hot fluid is introduced at a constant inlet temperature of (60 ^{o}C) and a constant flow rate of 7 L/m into the shell of the heat exchanger. Eight thermocouples were inserted at the entrance and exit of the heat exchanger (each two thermocouples were inserted in one point place to ensure the accuracy of the results) to measure the heat temperatures of inlet and outlet of the cold and hot fluid streams. An external cooling cycle was used to cool down the outlet cold-fluid stream, which exits from the tubes of heat exchanger in order to return its temperature to the initial temperature. While, the hot loop tank contains a heater to heat up the water that flows inside the shell. The experimental system has been designed in such a way that shell and tube heat exchanger or double pipe heat exchanger can be used, in both parallel and counter flow characteristics of the coolant nanofluid. The complete system is very dynamic and easy to use. It should be noted that some of the system parts such as the heat

exchangers and the fluid tanks were completely insulated by thermal insulation material made of (PVC and Nitrile rubber).

To evaluate the performance of the experimental setup and for comparison, the experimental system was tested with distilled water before measuring the heat transfer characteristics of the Al_2O_3/water and TiO_2/water nanofluids.

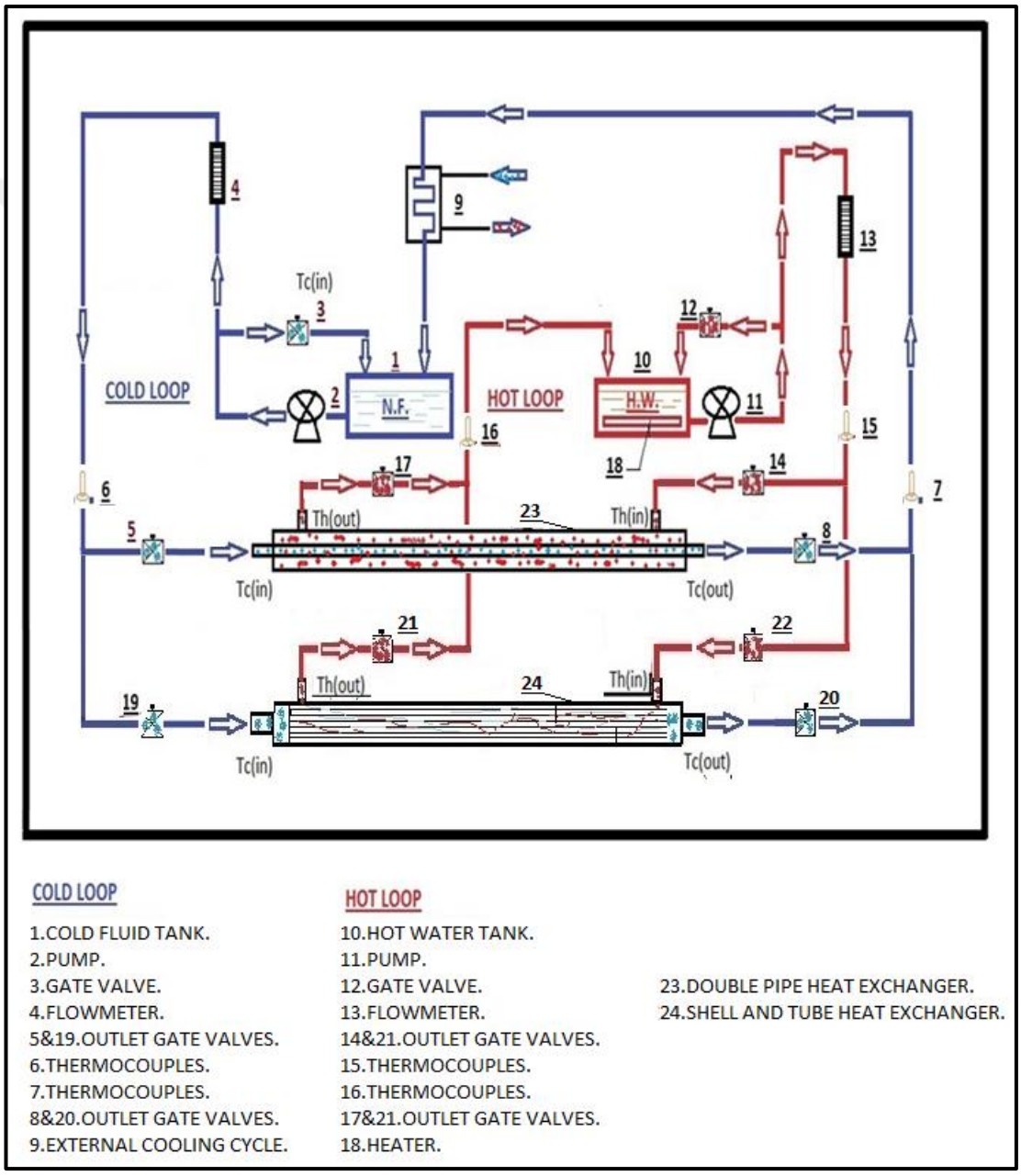

COLD LOOP

1.COLD FLUID TANK.
2.PUMP.
3.GATE VALVE.
4.FLOWMETER.
5&19.OUTLET GATE VALVES.
6.THERMOCOUPLES.
7.THERMOCOUPLES.
8&20.OUTLET GATE VALVES.
9.EXTERNAL COOLING CYCLE.

HOT LOOP

10.HOT WATER TANK.
11.PUMP.
12.GATE VALVE.
13.FLOWMETER.
14&21.OUTLET GATE VALVES.
15.THERMOCOUPLES.
16.THERMOCOUPLES.
17&21.OUTLET GATE VALVES.
18.HEATER.

23.DOUBLE PIPE HEAT EXCHANGER.
24.SHELL AND TUBE HEAT EXCHANGER.

Figure (3.1): The schematic diagram of the shell and tube experimental setup.

Figure (3.2): A photo of the experimental set-up.

3.1.1 Shell and Tube Heat Exchanger Set-up

The shell and tube heat exchanger was designed in such a way that, both parallel and counter flow characteristics of the coolant water or nanofluid could be analyzed. The outer shell is made of galvanized iron (GI) with an inner diameter of (57 mm) and outer diameter of (60 mm). The heat exchanger contains (9) tubes, which are made of copper with an inner diameter of (4.826 mm) and outer diameter of (6.35 mm) with (370 mm) in length as shown in Figure (3.3) and Table (3.1).

Figure (3.3): The shell and tube hear exchanger.

Table (3.1): The specification of shell and tube heat exchanger components.

Component	Dimension	Remark
The Shell	L = 410 mm L(test) = 370 mm D(in) = 57 mm D(out) = 60 mm	Metal : (GI) Pass = 1
The Tube	L = 37 mm D(in) = 4.826mm D(out) = 6.35 mm	Metal: Copper Number = 9

3.1.2 The Insulation Material

To minimize the heat loss, a thermal insulation material made of (PVC and Nitrile rubber) was used as shown in Figure (3.4). The insulation materials has a thickness of (1 cm), thermal conductivity of (0.034) W/m.K, and the temperature range of [(-38) °C to (+180) °C)]. It was used to insulate shell and tube heat exchanger, the storage tanks, and the inlet and outlet pipes, which were connected to the heat exchanger.

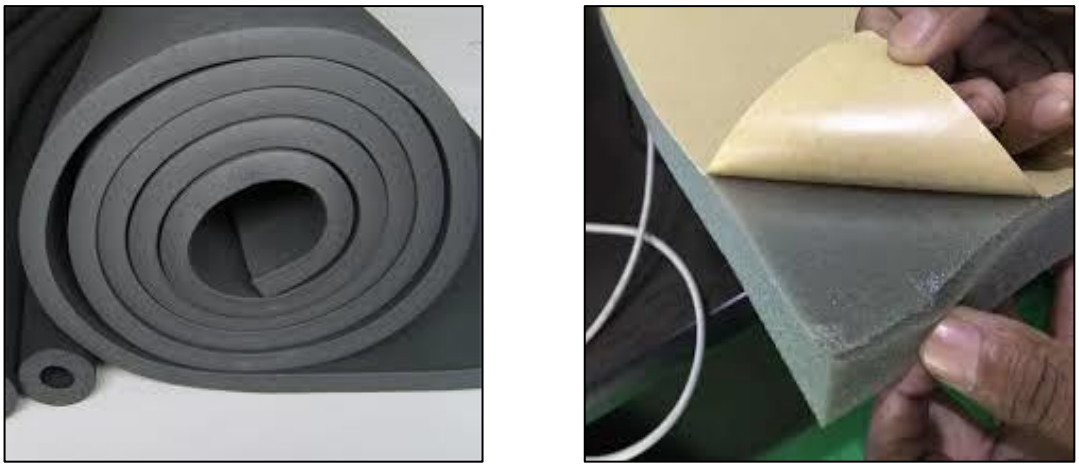

Figure (3.4): The thermal insulation material.

3.1.3 Pumps

The experimental system includes two pumps. The first one is installed in the hot loop with a single speed work, voltage of (220 V), frequency of (50 Hz) and heat resistant as shown in Figure (3.5). On other side, Figure (3.6) shows the cold-fluid loop pump with a single speed work, voltage of (220 V), and frequency of (50 Hz). These pumps were used to maintain a continuous flow for the closed cold and hot loops of the heat exchanger.

Figure (3.5): The hot water pump.

Figure (3.6): The cold fluid pump.

3.1.4 Storage Tanks

The system consists of two tanks. One of them is for the cold fluid and another one for the hot water. Figure (3.7) shows the storage tank of hot water. This tank has 15 liter capacity is made of stainless steel. The tank has a 2 kW electrical heater with automatic heat regulator in order to maintain a constant hot water temperature, and it is thermally insulated. Figure (3.8) shows the 20 liters storage tank of cold fluid that is made of plastic with slope base to prevent stagnation of Nanopowder.

Figure (3.7): The hot water tank.

Figure (3.8): The cold fluid tank.

3.2 The Measuring Devices

3.2.1 Thermocouples and thermometers

The inlet and outlet temperatures of hot water and cold fluid are measured using k-type thermocouples, which are inserted directly into the inlet and outlet flow stream of the heat exchanger. Readings of the thermocouples were recorded through a temperature recorder [(Thermocouple Thermometers)-(model HT-9815)-(made in China)] with 4 channels as shown in Fig. (3.9).The product specifications are:-

1 - Temperature range: - (-200$^{\circ}C$ ~ 1372$^{\circ}C$) (-328$^{\circ}F$ ~2501$^{\circ}F$)

2 - Accuracy :->100$^{\circ}C$ (-148$^{\circ}F$): ± 1°C (± 1°F) < 100$^{\circ}C$ (-148$^{\circ}F$): ± 2°C (± 3.6°F).

3 - Type K temperature resolution: < 1000$^{\circ}C$: < 0.1$^{\circ}C$/ ˚F < 1000$^{\circ}C$: < 1$^{\circ}C$/ ˚F/K.

Figure (3.9): The temperature recorder.

3.2.2 Flowmeters

There are two flowmeters incorporated in the experimental setup. The flow meter in Fig. (3.10) was used to measure the flow rate of hot water that flows in the heat exchanger shell. The range of this flow meter is 1.8 - 18 Lpm with an accuracy of ±5%. Figure (3.11) shows the flow meter that was used to measure the flow rate of cold fluid inside the heat exchanger tubes. The range of this flow meter is 0.5 - 8 Lpm with an accuracy of ±5%.

Figure (3.10): The flowmeter of hot loop.

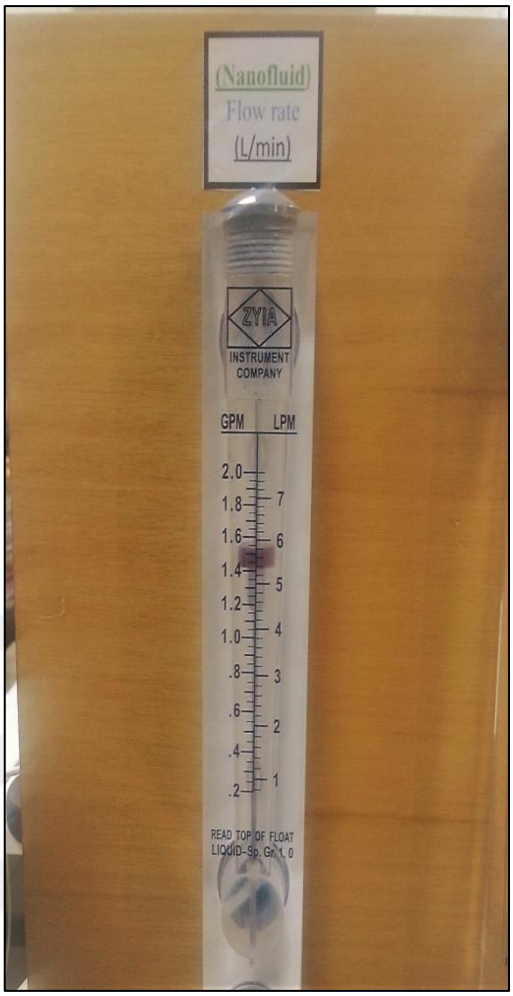

Figure (3.11): The flowmeter of cold loop.

3.3 The Calibration of Measuring Devices

Before proceeding with the experiments, all measuring devices were calibrated as described in the following sections:

3.3.1 Calibration of Thermocouples

All thermocouples were calibrated by connecting one end of thermocouple to digital thermometer and the other end inside de-ionized water in order to check the temperature that records at the boiling point. The water was placed in a bowl, then a heat source was focused on the bowl, when the water began to boil, the thermocouples were immersed in the boiling water to measure the temperature of

water in boiling state. As known, the boiling degree of de-ionized water is (100°C), and the thermometers record (100°C) in this state. That is mean that the thermometers recorded right temperature. Finally, this method was used to calibrate the thermometers in good and easy way.

3.3.2 Calibration of Flowmeters

The used flow meters were calibrated using a graded glass cylinder and stopwatch. Volume flow rate of 5, 5.5, 6, 6.5 and 7 L/m are used in calibrating the flow meters according to the following steps: a volume of water is accumulated in the graded cylinder after passing through the flow meter, which reads 1 L/m during a known period of time recorded by the watch 60 seconds, then The volume flow rate is calculated by dividing the volume by time.

3.4 Nanofluids

Titanium oxide TiO_2/water and Aluminium Oxide Al_2O_3/water nanofluids were used as working fluids instead of the base fluid (water) in the shell and tube heat exchanger. These nanofluids (Al_2O_3 in Water, gamma, 22 % by wt, 28nm particle diameter and TiO_2 in Water, Rutile, 22 wt%, 25-45nm in diameter) as shown Figure (3.12) were supplied by Nanografi Company (Nanotechnology Computer Manufacturing and Consulting LTD./Middle East Technical University, Turkey-Ankara). The properties of these nano powders are listed in Table (3.2).

Table (3.2): The properties of Titanium oxide (TiO_2) and Aluminium oxide (Al_2O_3) Nano powders.

No.	Technical properties	Al_2O_3	TiO_2
1	Purity %	99.99	99.99
2	Average particle size (nm)	28	25-45
3	Specific surface area (m^2/g)	150	50
4	True density (kg/m^3)	3900	4500
5	Color	white	white
6	Morphology	nearly spherical	nearly spherical
7	Elemental Analysis	Ca: <25pp Fe: <80pp Cr: <4ppm Na : <70pp Mn : <3pp Co: <2ppm	Al : 0.003 Ca: 0.005 Si: 0.003 S : 0.005 Mg : 0.01 W: 0.01

Figure (3.12): The Al_2O_3 /water and TiO_2/water nanofluids supplied by Nanografi Company (Turkey).

In order to obtain the required concentrations of 0.001, 0.002 and 0.003 for these nanofluids, the equation (3.1) will be used to determine the volume of water that must be added [8]:

$$\text{Vol }\%(\phi) = \frac{\text{volume of nanopowder (Vn.p.)}}{\text{volume of water(Vw)+volume of nanopowder (Vn.p.)}} \quad \ldots. (3.1)$$

Where:

Φ : Volume concentration of nanofluid.

$V_{n.p}$: Mass of Nanopowder / density of Nanopowder

V_w : Mass of water /density of water

After adding the required amount of distillated water to the concentrated nanofluid based on Eq. (3.1), the mixture was blended for one and half hour in a close cycle of nanofluid reservoir and water pump, as shown in Figure (3.13).

Figure (3.13): The nanofluid preparation

3.5 Experimental procedure

Before running the experiments, the following preparations were carried out as follows:

1. The tanks of the hot and cold fluids were filled with de-ionized water,

2. In the hot loop, the water was heated up to 60°C by the heater that fixed inside the hot fluid tank.

3. The thermocouples installed in their specified locations and connected to the temperature recorder.

4. The gate valves of the hot loop opened in order to allow the hot water to flow and saturate the heat exchanger in heating.

5. Checking all joints and fittings if there were leaking.

6. Preparing the proposed nanofluids in order to use.

7. Wearing gloves and medical mask to prevent touching the nanofluids or breathing its steam.

3.5.1 The Base Fluid Experiments

The deionized water was used as a reference cold fluid, which is introduced inside the tubes of shell and tube heat exchanger setup at flow rates of 5, 5.5, 6, 6.5 and 7 L/m. The hot water was pumped to shell and tube heat exchanger at a constant flow rate of 7 L/m and a constant temperature of 60 ^{o}C. Then, the valve gate of the cold fluid loop was opened, and the cold water was pumped inside the tube of the heat exchanger under a counter flow conditions. The flow rate of the cold fluid can be controlled by adjusting the get valve to get the required flow rate. Later on, the external cooling cycle was turned on and calibrated to keep the inlet cold-water temperature at 30°C. During the experiments, the temperatures of inlets and outlets of the heat exchangers were recorded. This experiment was repeated under the same operating conditions, but with different flow rates of 5, 5.5, 6, 6.5 and 7 L/m of the cold loop. There is a very important observation; these procedures were repeated at least three times for each experiment of each flow rate value in order to get the most accuracy results for each one of them.

3.5.2 The TiO_2/water nanofluids experiments

The base fluid (water) of the cold loop was replaced by TiO_2/water nanofluid. At the beginning, the TiO_2/water nanofluid with volume concentration of 0.1% was used as a working fluid at different flow rates of 5, 5.5, 6, 6.5 and 7 L/m. Then, the results were compared to those of the base fluid at the same conditions. The experiment was repeated in same way for the concentrations of 0.2% and 0.3%.

3.5.3 The Al_2O_3/water nanofluids experiments

The cold fluid loop was emptied form the TiO_2/water nanofluid and washed by water to remove the residue of TiO_2/water nanofluid. The tank of cold fluid loop was refilled with the Al_2O_3/water nanofluid, and the same experiments of base fluid and TiO_2/water nanofluid were performed for the Al_2O_3/water nanofluids with different concentrations of 0.1%., 0.2% and 0.3%. For each concentration, the flow rate was varied within the range of 5, 5.5, 6, 6.5 and 7 L/m, and the inlet and outlet temperatures of the cold and hot fluids were recorded.

3.5.4 The Final Experiments

The schematic of the experiments is shown in Figure (3.14). It contains a summary of the experiments under counter flow pattern for a constant hot water flow rate of 7 L/m for all experiments.

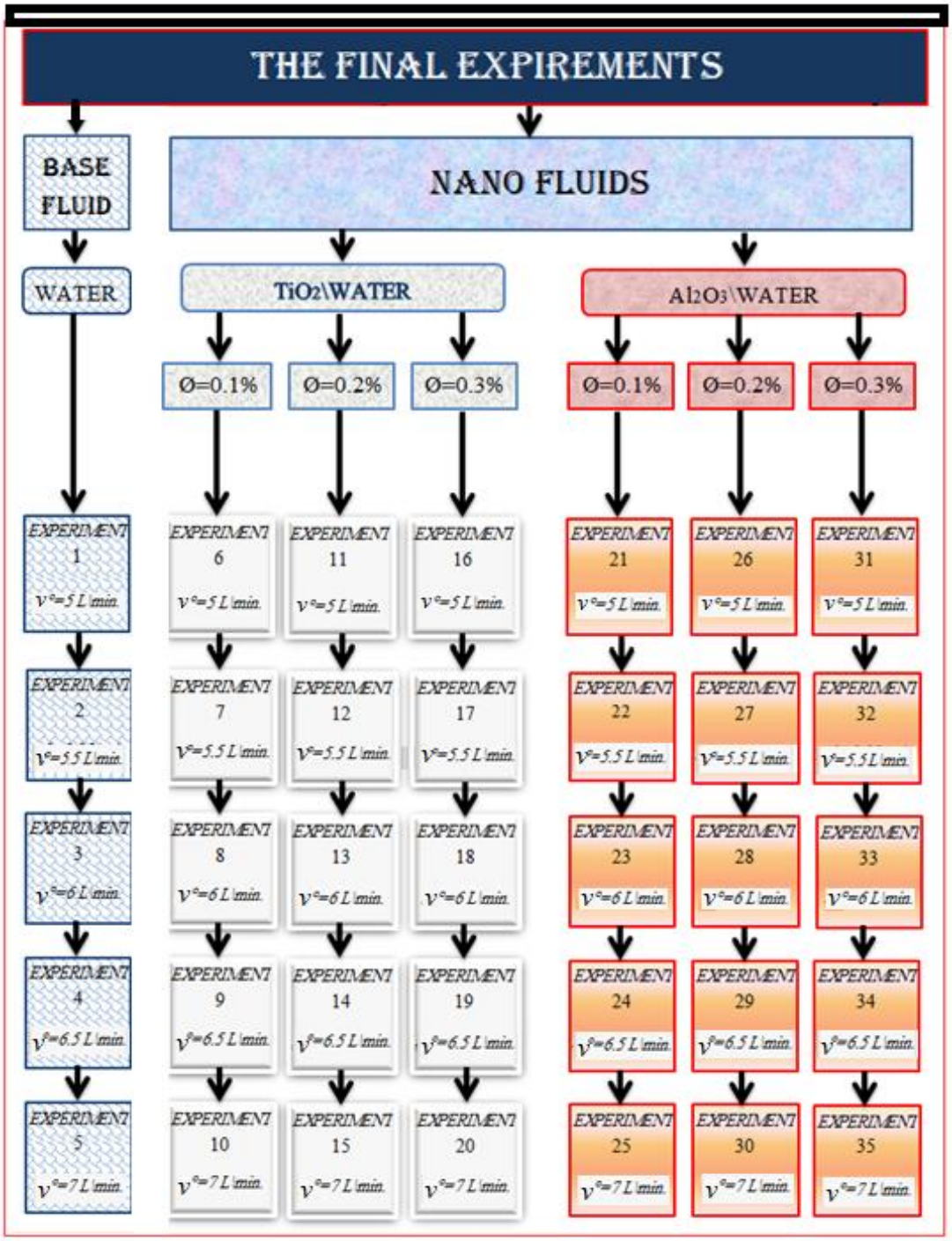

Figure (3.14): The schematic of the experiments.

3.5.5 Theoretical Analysis

The total heat transfer of the shell and tube heat exchanger for water can be calculated by equation (3.2) [9]:

$$Q_b = \dot{m}_b \times C_{p.b} \times (T_{b.out} - T_{b.in}) \quad \ldots. (3.2)$$

Where:

$\dot{m}_b$ Mass flow rate of base fluid, L/s

$Cp._b$ Specific heat of base fluid, J/kg K

$T_{b.out}$ Outlet temperature of base fluid, °C

$T_{b.in}$ Inlet temperature of base fluid, °C

The properties of water are determined at average temperature (mean temperature) which calculated by equation (3.3) [25][25]:

$$T_m = \frac{(T_{out} + T_{in})}{2} \quad \ldots. (3.3)$$

The water velocity inside the shell and inside the tube can be expressed by equation (3.4) [25]:

$$V = \frac{V^{\circ}}{A_c} \quad \ldots. (3.4)$$

$$V^{\circ} = \frac{\dot{m}}{\rho} \quad \ldots. (3.4.a)$$

$$A_c = \frac{\pi}{4} d_{in}^2 \quad \ldots. (3.4.b)$$

Where:

ρ Density, kg/m^3

A_c Cross section area, m^2

d_i Tube inner diameter, m

V Inside mean velocity, m/s

V° Volume flow rate

The Reynolds number is defined as in equation (3.5) [25]:

$$R_e = \frac{\rho V_{in} d_i}{\mu} \quad \text{…. (3.5)}$$

$$\mu = v \, x \, \rho \quad \text{…. (3.5.a)}$$

Where:

V_{in} Mean velocity (inside tube), m/s

d_i Tube inner diameter, m

μ Dynamic viscosity (kg/m.s)

v Kinematic viscosity, m^2/s

The Nusselt number for water is calculated by equation (3.6) [25]:

$$Nu = \frac{h D}{K} \quad \text{.... (3.6)}$$

Where:

h Heat transfer coefficient, W/m^2 k

K Conductivity, W/m.k

The Nusselt number for water is calculated by equation (3.7) [25]:

$$Nu = 0.012(Re^{0.8} - 280)Pr^n \quad \text{…. (3.7)}$$

The properties in this equation are evaluated at the average fluid bulk temperature, and the exponent *n* has the following values:

n = 0.4 for heating of the fluid

n = 0.3 for cooling of the fluid

For: 1.5<Pr <500, 3000<Re<10^6

The overall heat transfer coefficient for nanofluids and water is expressed by the equations (3.8) and (3.9) [9]:-

$$U_{\mathrm{i}} = \frac{Q}{A_s \, x \, \Delta T_{lm}} \quad \text{…. (3.8)}$$

$$Uinf = \frac{Q_{nf}}{A_s \, x \, \Delta T_{lm}} \quad \text{…. (3.9)}$$

Where:

ΔT_{lm} The logarithmic mean temperature difference °C:

$$\Delta T_{lm} = \frac{(T_{h2}-T_{c2})-(T_{h1}-T_{c1})}{Ln\frac{(T_{h2}-T_{c2})}{(T_{h1}-T_{c1})}} \quad \text{…. (3.8.a)}$$

The thermophysical properties of the nanofluid were calculated and based on mean bulk temperature. The heat transfer rate of the nanofluid is:

$$Q_{nf} = m^{\circ}_{nf} \, . C_{p.nf}(T_{o.nf} - T_{i.nf}) \quad \text{…. (3.10)}$$

Where:

m°_{nf} Mass flow rate of nanofluid, L/s

$C_{p.nf}$ Specific heat of nanofluid, J/kg K

$T_{o.nf}$ Outlet temperature of nanofluid, °C

$T_{i.nf}$ Inlet temperature of nanofluid, °C

The equation that is appropriate for using nanofluid density is (3.11) [9]:

$$\rho_{nf} = (1 - \phi)\rho_{bf} + \phi\rho_{np} \quad \text{…. (3.11)}$$

Where:

ρ_{np} Density of Nanopowder, kg/m^3

ρ_{bf} Density of base fluid, kg/m^3

ϕ The concentration of nanofluid, %

In addition, the specific heat of nanofluid can be determined by the equation (3.12) [9]:

$$C_{p,nf} = \frac{(1-\phi)\rho_{bf}C_{p.bf}+\phi\rho_{np}C_{pnp}}{\rho_{nf}} \quad \text{…. (3-12)}$$

Where:

$C_{p.bf}$ The specific heat of base fluid, J/kg K

C_{pnp} The specific heat of Nanopowder, J/kg K

The dynamic viscosity of nanofluids was calculated by the equation (3.13) [9]:

$$\mu_{nf} = \mu_{bf}(1 + 2.5\ \emptyset\ ) \quad \text{…. (3.13)}$$

Where (μ) is the dynamic viscosity and the subscripts (p), (bf)and (nf) refer to particle, base fluid, and nanofluid, respectively.

The effective thermal conductivity (K_{nf}) of the nanofluids can be evaluated by equation (3.14) [9]:

$$k_{nf} = k_{bf}\left[\frac{k_{np}+2k_{bf}-2\phi(k_{bf}-k_{np})}{k_{np}+2k_{bf}+\phi(k_{bf}-k_{np})}\right] \quad \text{…. (3.14)}$$

Where (k) is the effective thermal conductivity and the subscripts (np), (bf)and (nf) refer to nano particles, base fluid, and nanofluid, respectively.

The Reynolds and Prandtl numbers are calculated with considering the nanofluid properties as follows by equation (3.14) and (3.15) [9]:

$$Re_{nf} = \frac{\rho_{nf}\, u_{nf}\, D_{h.nf}}{\mu_{nf}} \quad \text{…. (3.14)}$$

$$Pr_{nf} = \frac{C_{p_{nf}}\, \mu_{nf}}{K_{nf}} \quad \text{…. (3.15)}$$

The following equations (3.16) and (3.17) were used to predict the Nusselt number of the nanofluids [8]:

$$Nu_{nf} = 0.074 {Re_{nf}}^{0.707} {Pr_{nf}}^{0.385} \emptyset^{0.074} \quad \text{…. (3.16)}$$

$$Nu_{nf} = \frac{h_{i.nf}\, d_i}{K_{nf}} \quad \text{…. (3.17)}$$

According to the equation (3.17), the heat transfer coefficient for the nanofluids is expressed by the equation (3.18):

$$h_{i.nf} = \frac{Nu_{nf}\, K_{nf}}{d_i} \quad \text{…. (3.18)}$$

The calculated thermophysical properties of the nanofluids were listed in Table (3.3).

Table (3.3): Thermophysical properties of the base fluid and nanoparticles.

No.	Property	Al_2O_3 (nanoparticles)	TiO_2 (nanoparticles)	Water (base fluid)
1	$c_p[J.kg^{-1}.k^{-1}]$	895	689.36	4178
2	$\rho[kg.m^{-3}]$	3900	4500	996
3	k$[W.m^{-1}.K^{-1}]$	36	8.4	0.617
4	$d_p(nm)$	28	25-45	-

CHAPTER FOUR

RESULTS AND DISCUSSION

The experimental heat transfer results of the proposed nanofluids (TiO_2\water and Al_2O_3\water) as well as the results of base fluid in the shell and tube heat exchanger were presented and discussed in this chapter. The results of these nanofluids are evaluated based on the effect of varying volume concentrations of 0.1, 0.2 and 0.3% of each kind of nanofluids, and flow rates of 5, 5.5, 6, 6.5 and 7 L/m for each concentration of the proposed nanofluids on the performance of the heat exchanger. The shell and tube heat exchanger performance is expressed by the difference of the flowing fluids in the heat exchanger. The parameters of heat transfer, heat transfer coefficient, over all heat transfer coefficient, Reynolds number and Nusselt number were calculated according to the equations that were related with these situations. On the other hand, as it was mentioned in chapter three, the apparatus can be used for shell and tube heat exchanger experimental and for double pipe heat exchanger experimental. Two experimental collections were carried out on the same period. The present study carried out the first experimental collection on the shell and tube heat exchanger, and another one carried out the second experimental collection on the double pipe heat exchanger by Mr. Mohanad AL-SAMMARRAIE in a study title of HEAT TRANSFER PERFORMACE OF DOUBLE PIPE HEAT EXCHANGER USING Al_2O_3/WATER AND TiO_2/WATER NANOFLUIDS for same types of fluids and same concentrations of nanofluids that were used in the present study experimental, but in different flow rates of 2.5, 3, 3.5, 4 and 4.5 L/m [26]. Finally, the results of all present study experiments analyzed to create a comparison among them.

4.1 The effect of heat exchanger geometry

The weight and size of heat exchangers are very important parameters, and cost considerations are frequently subordinated insofar as material and heat-exchanger construction costs are concerned; however, the weight and size are important cost factors in the overall application in these fields and thus may still be considered as economic variables. A particular application will dictate the rules that one must follow to obtain the best design with economic considerations, size, weight, etc. [25]. Designing of heat exchanger is required to increase energy saving. Heat exchanger geometry is very important, and it was characterized by a high surface area per unit volume, which can result high efficiency heat exchanger [1].

In shell and tube heat exchanger, increasing velocity by increasing mass flow rate, increasing active surface area, increasing number of tubes, the kind of pipes metal and cross section area are very important to get high heat transfer coefficients, Reynolds number and overall heat transfer coefficient, which may be sufficient to improve Heat exchanger performance. Finally, Heat exchanger enhancement effected with inserts, coiled or twisted tubes, surface treatments, and additives [3].

4.2 Preparation and assembly of the test apparatus

In order to conduct this study, it must work to manufacture a new experimental system, Because of the lack of such a device in the university for these types of experiments. The first step is manufacturing shell and tube heat exchanger. In the middle of April 2017, shell and tube heat exchanger was manufactured according to the thesis requirements in a specialized workshop. After that, all the other devices and auxiliaries were bought from the component markets that were specialized to sell these kinds of equipment. The assembling of the test system was carried out in the laboratory of the aerodynamic department of the university of Turkish aeronautical association institute of science and technology in Ankara under eyes of Assist. Prof. Dr. Mohamed Salem Elmnefi “the supervisor of this thesis”.

The set-up of the system was got duration from the middle of April to the end of June 2017. In this period, the proposed Nano fluids were prepared in the

laboratory of the Nanografi Company of the Middle East University in Ankara-Turkey. Finally, the system was completed and be ready to use on 30 June 2017.

4.3 Experimental Results

Although the devices of measuring were calibrated, but this calibration does not enough to prevent the existence of a simple error in reading temperature because of the difference between the response time of the device and the period of change in temperature in the point which required to measure. Therefore, the procedures were repeated at least three times for each experiment of each flow rate value, and the average of the results were approved in order to get the best accuracy results for each one of them. Moreover, the standard deviation and standard error value for each experiment temperatures were calculated.

The standard deviation "provides a sort of average of the differences of all scores from the mean", and it is associated to the range. A low standard deviation means that a set of scores is not very widely dispersed around the mean, while a high standard deviation indicates that the scores are more widely dispersed. The standard deviation of such a distribution of means is referred to as the standard error of the mean because it represents the distribution of errors in estimating temperature. Thus, the standard error of the mean is the standard deviation for the distribution of errors [27]. The standard deviation is often denoted by the Greek letter sigma, σ. For a finite number of measurements, *Xi*, the standard deviation is given by[28][28]:

$$\sigma = \left[\frac{1}{n-1}\sum_{i-1}^{n}(Xi - \bar{X})^2\right]^{\frac{1}{2}} \qquad \text{..... (4.1)}$$

Where:

$\bar{X}$ Mean temperature.

n Number of the tests.

The standard error is a statistical indicator of the reliability of a descriptive statistic estimated from a sample. The standard error represents the typical amount of error that can be expected from an estimator. Hence, the smaller the standard error, the better the estimate is likely to be. The standard error S.E. is given by [27]:

$$S.E. = \frac{\sigma}{\sqrt{n}} \quad \text{.... (4.2)}$$

4.3.1 Base fluid (water) Experimental Results

The first experiment on the base fluid (water) as a cooling fluid was carried out on 9 July 2017, in flow rates of 5, 5.5, 6, 6.5 and 7 L/m and inlet shell and tube heat exchanger temperature of 30 °C for the cold loop (inside tubes), and flow rate of 7 L/m and inlet shell and tube heat exchanger temperature of 60 °C for the hot water of the hot loop (inside shell). Table (4.1) declares the inlet and outlet temperatures of the base fluid which was flowed in shell and tube heat exchanger which measured by thermocouples for three times, the flow rates of the base fluid which were flowed inside the tubes which measured by the flowmeter of the cold loop, standard deviation and standard error.

Table (4.1): The temperature and flow rates of using water.

NO.	Type of fluid	Total Flow Rate (V°) (L /m)	T inlet °C	Toutlet Test 1 °C	Toutlet Test 2 °C	Toutlet Test 3 °C	Toutlet Avarage Test °C	Standard Deviation	Standard Error	DATE
	COLD LOOP (INSIDE TUBES)									
1	water	5.0	30.0	33.1	33.2	33.1	33.13	0.05774	0.03333	9-Jul-2017
2	water	5.5	30.0	32.9	33.0	32.9	32.93	0.05774	0.03333	
3	water	6.0	30.0	32.8	32.7	32.7	32.73	0.05774	0.03333	
4	water	6.5	30.0	32.6	32.5	32.6	32.57	0.05774	0.03333	
5	water	7.0	30.0	32.4	32.4	32.5	32.43	0.05774	0.03333	

Figure (4.1) declares the relation between the average temperature with each amount of flow rates and the standard error for the average temperature. The small value of the standard error confirms the approximate value of the temperature (average temperature) in each experiment to the true value.

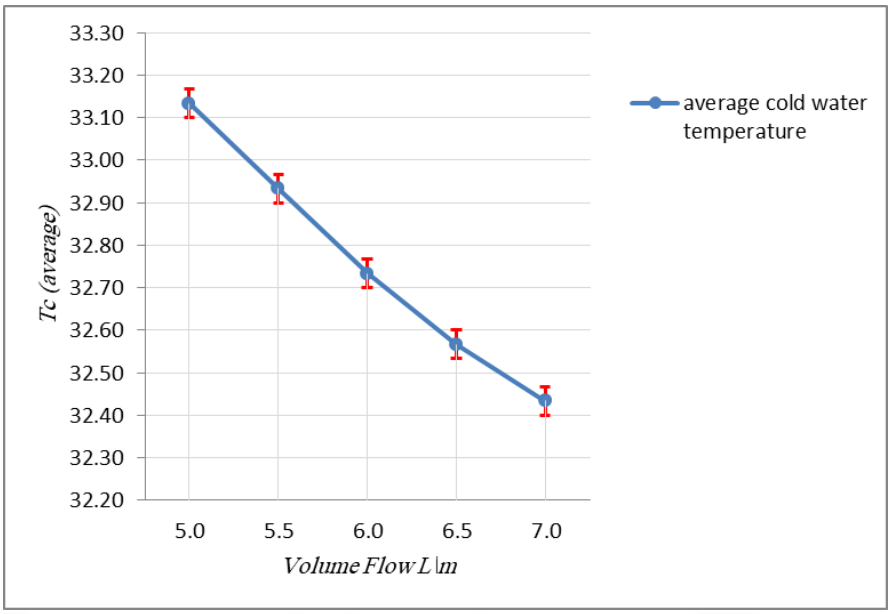

Figure (4.1): The graph of ($T_{av.}$ VS V°), for (Water) and the standard error.

4.3.2 TiO_2 \ Water nanofluids Experimental Results

The next experiment on the TiO_2\water nanofluid with TiO_2 nanoparticles of 0.1% was introduced to shell and tube heat exchanger instead of cold water to study its effect on the performance of heat exchanger. This experiment was performed on 16 july2017, and repeated for two times for the same nanofluid, but for concentrations of 0.2 and 0.3% at the same conditions mentioned previously on 24 and 31 July 2017, respectively. Table (4.2) presents the inlet and outlet temperatures of the base fluid which was flowed in shell and tube heat exchanger which measured by thermocouples for three times, the flow rates of TiO_2\water nanofluid in three concenrations which were flowed inside the tubes which measured by the flowmeter of the cold loop, standard deviation and standard error.

Table (4.2): The temperatures and the flow rates of using TiO_2\water nanofluids.

NO.	Type of nano fluid	Total Flow Rate (V°) (L /m)	Concentration Ø (N.P.) (%)	T inlet °C	Toutlet Test 1 °C	Toutlet Test 2 °C	Toutlet Test 3 °C	Toutlet Avarage Test °C	Standard Deviation	Standard Error	DATE
	COLD LOOP (INSIDE TUBES)										
1	TiO2\water	5.0	0.1	30.0	33.4	33.5	33.5	33.47	0.05774	0.03333	16-Jul-17
2		5.5	0.1	30.0	33.3	33.2	33.4	33.30	0.05774	0.03333	
3		6.0	0.1	30.0	33.0	33.1	33.1	33.07	0.05774	0.03333	
4		6.5	0.1	30.0	33.0	32.9	32.9	32.93	0.05774	0.03333	
5		7.0	0.1	30.0	32.8	32.7	32.8	32.77	0.05774	0.03333	
6	TiO2\water	5.0	0.2	30.0	33.6	33.5	33.6	33.57	0.05774	0.03333	24-Jul-17
7		5.5	0.2	30.0	33.4	33.5	33.5	33.47	0.05774	0.03333	
8		6.0	0.2	30.0	33.3	33.4	33.3	33.33	0.05774	0.03333	
9		6.5	0.2	30.0	33.1	33.1	33.2	33.13	0.05774	0.03333	
10		7.0	0.2	30.0	33.0	32.9	33.0	32.97	0.05774	0.03333	
11	TiO2\water	5.0	0.3	30.0	33.8	33.9	33.9	33.87	0.05774	0.03333	31-Jul-17
12		5.5	0.3	30.0	33.6	33.7	33.7	33.67	0.05774	0.03333	
13		6.0	0.3	30.0	33.5	33.5	33.6	33.53	0.05774	0.03333	
14		6.5	0.3	30.0	33.4	33.5	33.4	33.43	0.05774	0.03333	
15		7.0	0.3	30.0	33.3	33.3	33.3	33.30	0.05774	0.03333	

Figure (4.2) declares the relation between the average temperature with each amount of flow rates and the standard error for the average temperature, for each concentration.

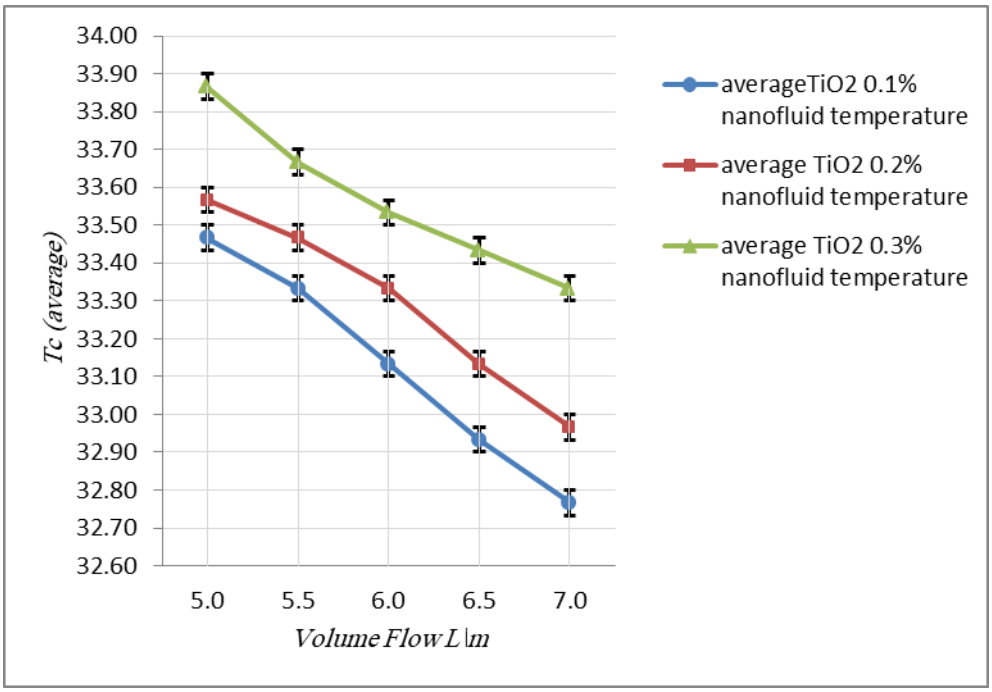

Figure (4.2): The graph of ($T_{av.}$ VS V°), for (TiO_2 0.1, 0.2 & 0.3%) and the standard error.

4.3.3 Al_2O_3\ water nanofluids Experimental Results

In August, another three experiments were carried out on the Al_2O_3\ water nanofluids instead of TiO_2\water nanofluids that used in the previous experiments, and with concentrations of 0.1, 0.2 and 0.3% at the same initial conditions mentioned in all previous experiments. These experiments were performed on 7, 15 and 21 August 2017, respectively. Table (4.3) presents the inlet and outlet temperatures of the base fluid which was flowed in shell and tube heat exchanger which measured by thermocouples for three times, the flow rates of Al_2O_3\water nanofluid in three concentrations which were flowed inside the tubes which measured by the flowmeter of the cold loop, standard deviation and standard error.

Table (4.3): The temperatures and the flow rates of using Al_2O_3\water nanofluids.

NO.	Type of nano fluid	Total Flow Rate (V°) (L /m)	Concentration Ø (N.P.) (%)	T inlet °C	Toutlet Test 1 °C	Toutlet Test 2 °C	Toutlet Test 3 °C	Toutlet Avarage Test °C	Standard Deviation	Standard Error	DATE
	COLD LOOP (INSIDE TUBES)										
1	Al2O3\water	5.0	**0.1**	30.0	33.6	33.5	33.5	33.53	0.05774	0.03333	07-Aug-17
2		5.5	**0.1**	30.0	33.4	33.3	33.4	33.37	0.05774	0.03333	
3		6.0	**0.1**	30.0	33.2	33.3	33.3	33.27	0.05774	0.03333	
4		6.5	**0.1**	30.0	33.1	33.2	33.2	33.17	0.05774	0.03333	
5		7.0	**0.1**	30.0	33.0	33.1	33.1	33.07	0.05774	0.03333	
6	Al2O3\water	5.0	**0.2**	30.0	33.9	33.9	34.0	33.93	0.05774	0.03333	15-Aug-17
7		5.5	**0.2**	30.0	33.8	33.8	33.9	33.83	0.05774	0.03333	
8		6.0	**0.2**	30.0	33.8	33.7	33.7	33.73	0.05774	0.03333	
9		6.5	**0.2**	30.0	33.6	33.6	33.5	33.57	0.05774	0.03333	
10		7.0	**0.2**	30.0	33.5	33.6	33.5	33.53	0.05774	0.03333	
11	Al2O3\water	5.0	**0.3**	30.0	34.0	34.1	34.1	34.07	0.05774	0.03333	21-Aug-17
12		5.5	**0.3**	30.0	34.0	34.1	34.0	34.03	0.05774	0.03333	
13		6.0	**0.3**	30.0	33.8	33.7	33.8	33.77	0.05774	0.03333	
14		6.5	**0.3**	30.0	33.7	33.7	33.8	33.73	0.05774	0.03333	
15		7.0	**0.3**	30.0	33.6	33.6	33.6	33.60	0.05774	0.03333	

Figure (4.3) declares the relation between the average temperature with each amount of flow rates and the standard error for the average temperature, for each concentration.

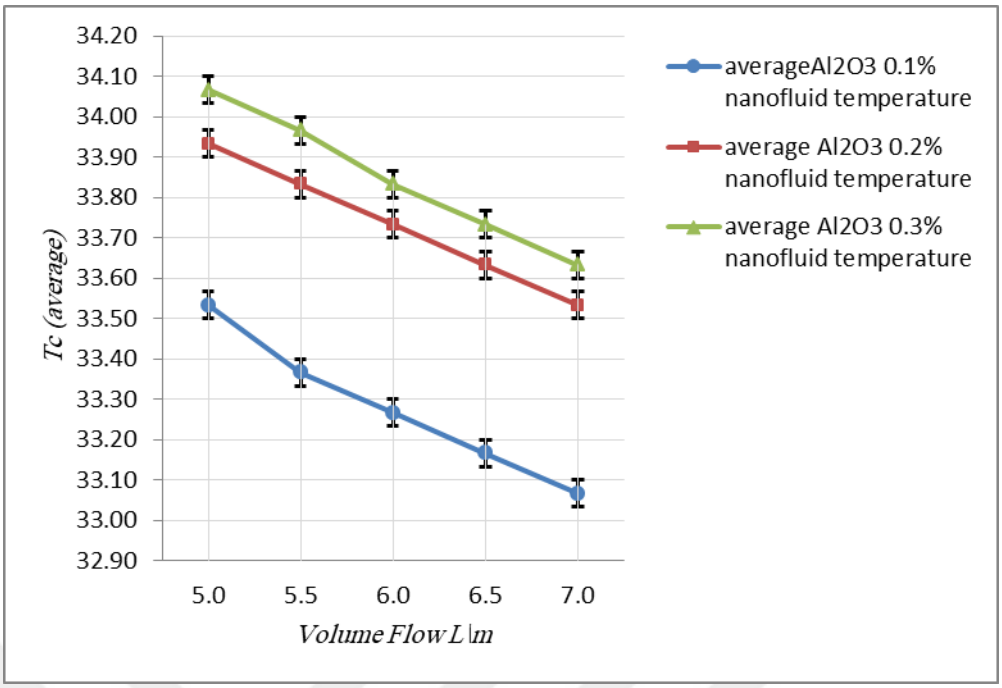

Figure (4.3): The graph of ($T_{av.}$ VS V°), for (Al_2O_3 0.1, 0.2 & 0.3%) and the standard error.

4.4 The performance results of the shell and tube heat exchanger

4.4.1 Heat transfer versus flow rate

Figure (4.4) shows the heat transfer enhancement ratio according to the flow rate of the cooling fluids. The ratio of Al_2O_3\water and TiO_2\water nanofluids heat transfer rate to the heat transfer rate of pure water, for nanoparticles concentrations of 0.1% for each of these nanofluids in flow rates of 5, 5.5, 6, 6.5 and 7 L\m, it was clear that the addition of nanoparticles to the base fluid increased the heat transfer rate, and it was clear that the effect of adding Al_2O_3 nanoparticles to the base fluid got better results than the effect of adding TiO_2 nanoparticles to the base fluid.

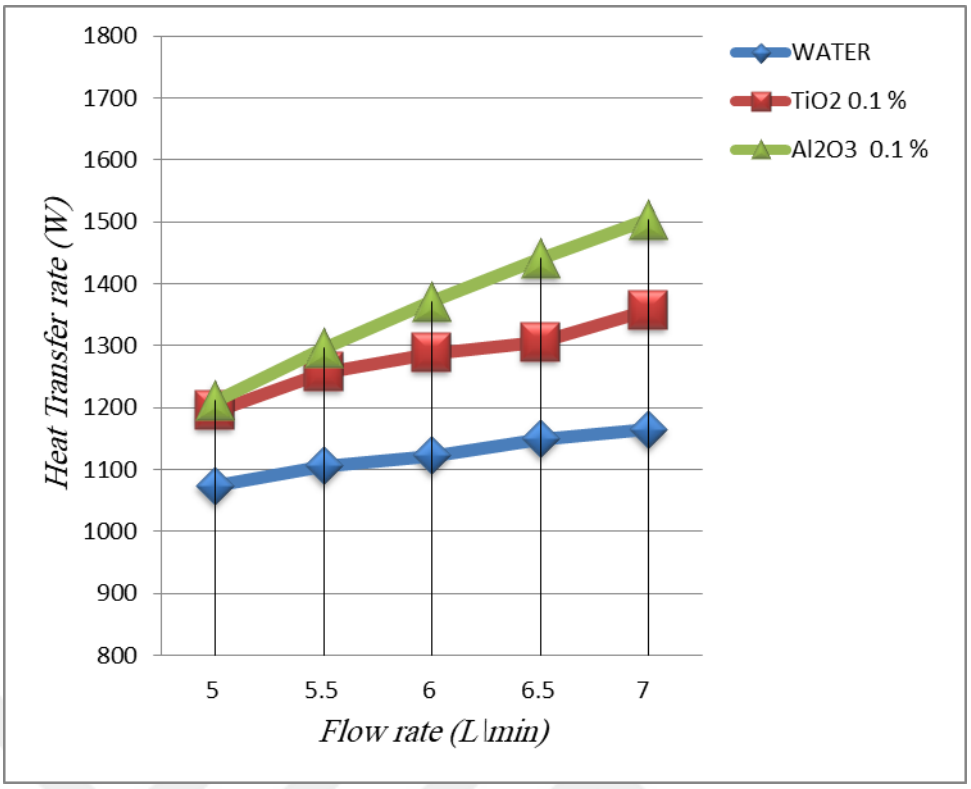

Figure (4.4): The graph of (Q VS V°), for (Water, TiO_2 0.1% & Al_2O_3 0.1%).

The heat transfer enhancement ratio is declared in figure (4.5) according to the flow rate of the cooling fluids of Al_2O_3\water, TiO_2\water nanofluids and water, for nanoparticles concentrations of 0.2% for the nanofluids in flow rates of 5, 5.5, 6, 6.5 and 7 L\m. The addition of nanoparticles to the base fluid increased the heat transfer rate, and the effect of adding Al_2O_3 nanoparticles to the base fluid got better results than the effect of adding TiO_2 nanoparticles to the base fluid.

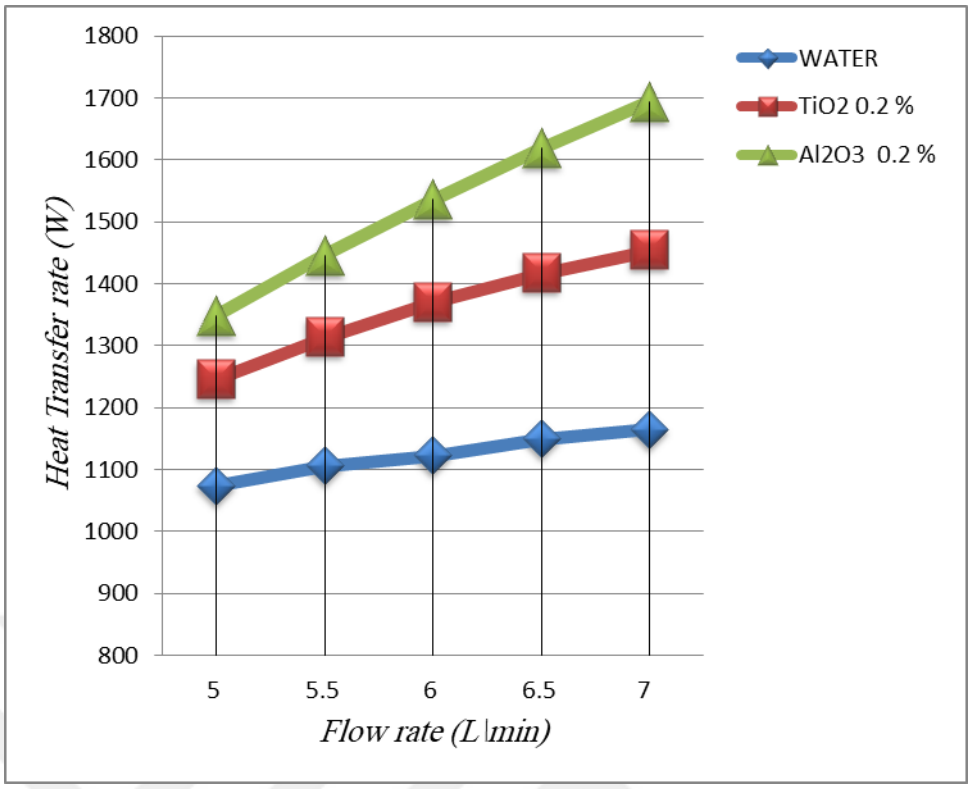

Figure (4.5): The graph of (Q VS V°), for (Water, TiO_2 0.2 % & Al_2O_3 0.2%).

The best heat transfer rate happened for Al_2O_3\water and TiO_2\water nanofluids in concentration of 0.3 % for each of nanofluids in flow rates of 5, 5.5, 6, 6.5 and 7 L\m. Furthermore, the heat transfer rate of Al_2O_3\water nanofluid was better than TiO_2\water nanofluid and water respectively, as shown in figure (4.6).

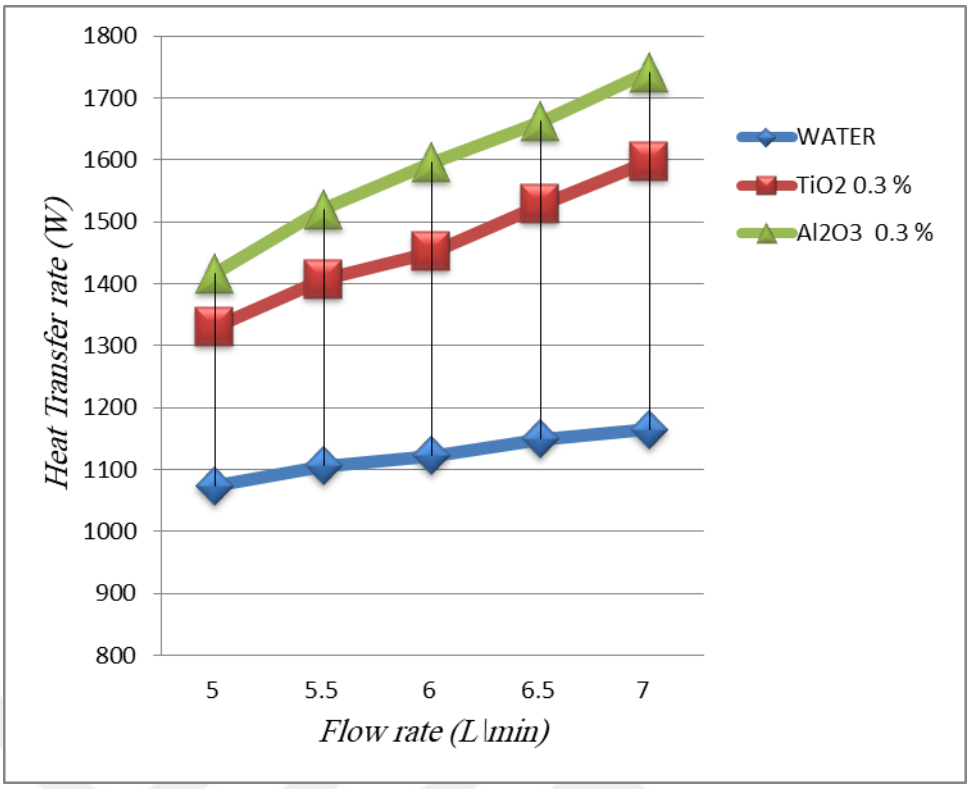

Figure (4.6): The graph of (Q VS V°), for (Water, TiO_2 0.3% & Al_2O_3 0.3%).

Figure (4.7) shows the comparison among water and Al_2O_3\water nanofluids in concentrations of (0.1, 0.2 and 0.3%) according to the flow rate of 5, 5.5, 6, 6.5 and 7 L\m. On the other hand, figure (4.8) shows the comparison among water and TiO_2\water nanofluid in concentrations of (0.1, 0.2 and 0.3%) according to the flow rate of 5, 5.5, 6, 6.5 and 7 L\m, too.

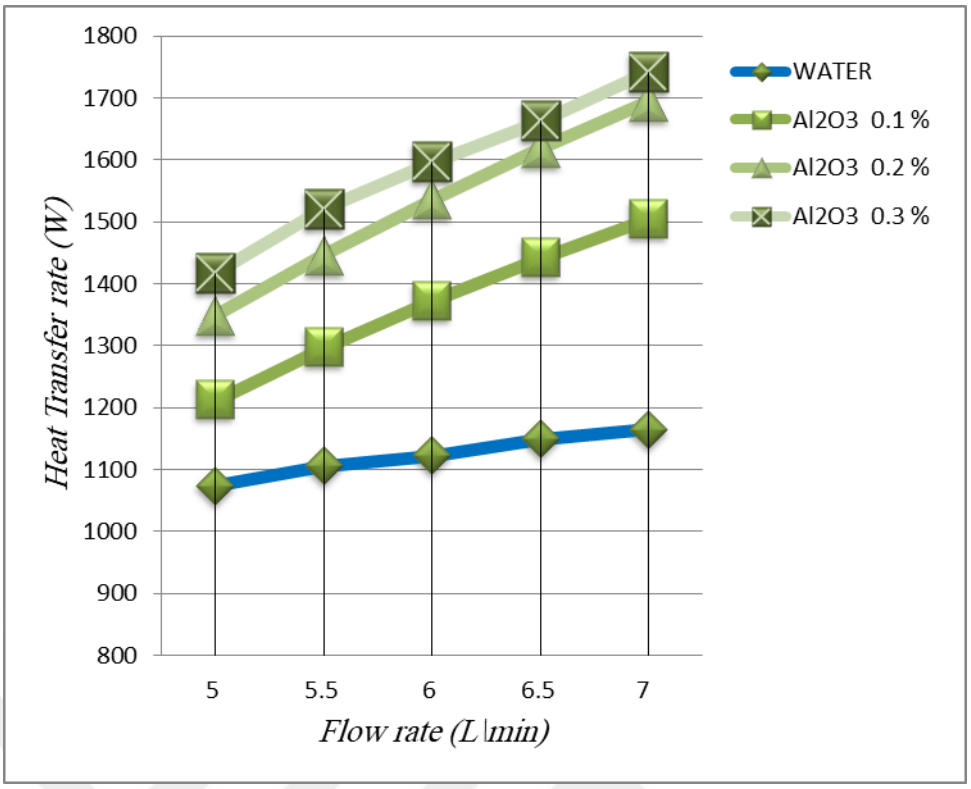

Figure (4.7): The graph of (Q VS V°), for (Water & Al_2O_3 0.1, 0.2 & 0.3%).

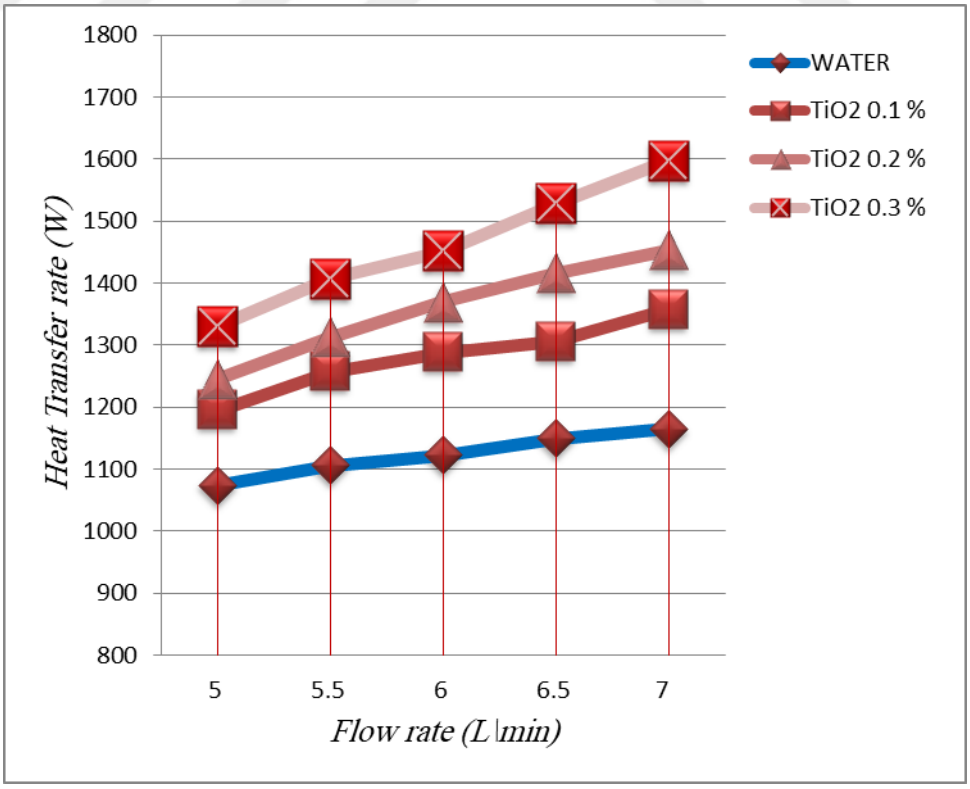

Figure (4.8): The graph of (Q VS V°), for (Water, TiO_2 0.1, 0.2 & 0.3%).

Through what was mentioned, The results and figures showed that the heat transfer rate was better in nanofluids than water, and it increases with the increase in volume concentration of the nanoparticles for a given mass flow rate, and it also increases with the increase in mass flow rate of cold fluid for a same volume concentration of the nano particles.

4.4.2 Overall heat transfer coefficient versus flow rate

The effect of adding nanoparticles to the water on the overall heat transfer coefficient for the volume concentration of 0.1%, for both Al_2O_3\water and TiO_2\water nanofluids, according to the flow rate of 5, 5.5, 6, 6.5 and 7 L\m was shown in figure (4.9).

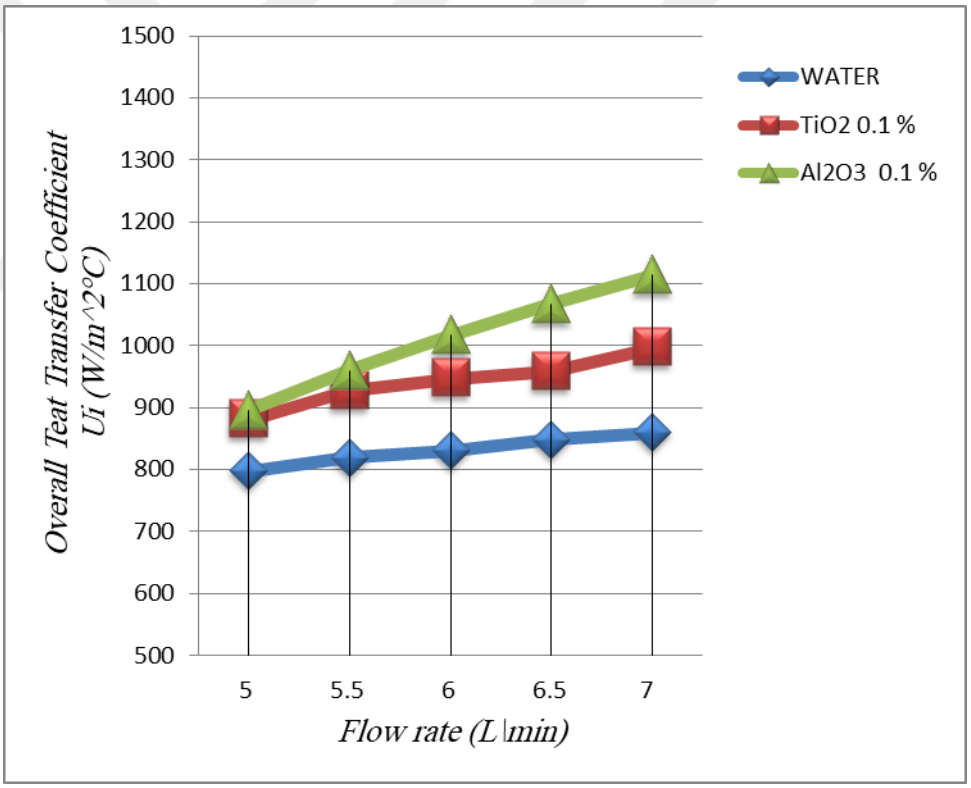

Figure (4.9): The graph of (Ui VS V°), for (Water, TiO_2 0.1% & Al_2O_3 0.1%).

The comparison of overall heat transfer coefficient for Al_2O_3\water, TiO_2\water nanofluids in volume concentration of 0.2% and water according to the flow rate of 5, 5.5, 6, 6.5 and 7 L\m is shown in figure (4.10). Figure (4.11) shows the results of same previews experiment, but this time it was done with volume

concentration of 0.3% for Al_2O_3\water, TiO_2\water nanofluids and water in a given flow rate of 5, 5.5, 6, 6.5 and 7 L\m.

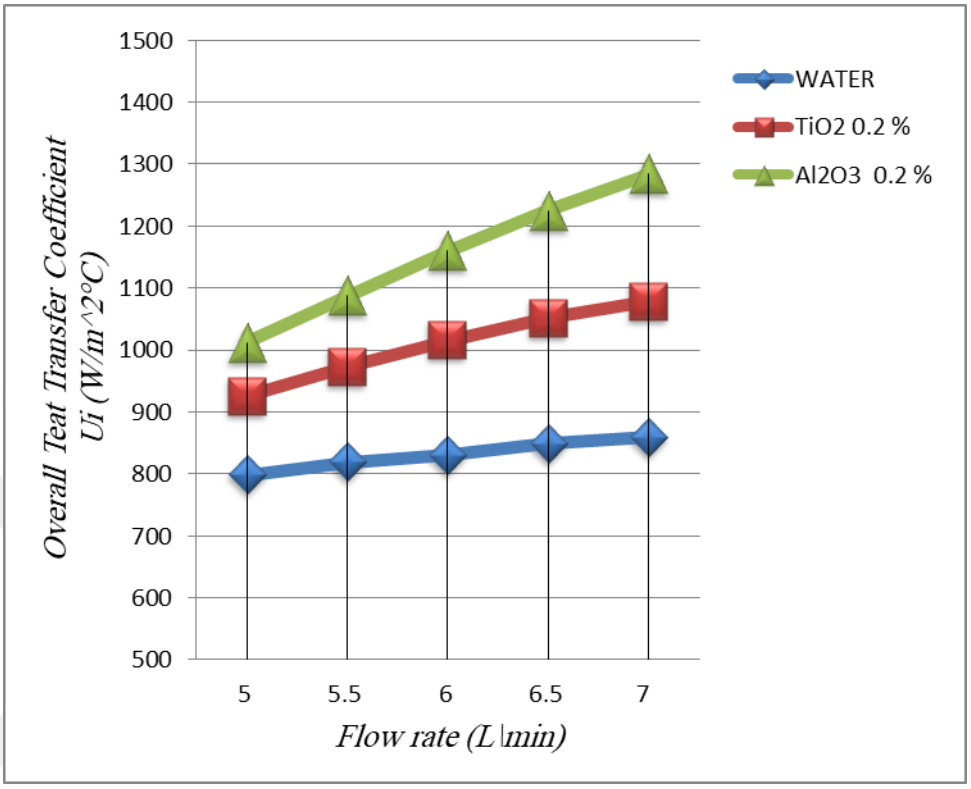

Figure (4.10): The graph of (Ui VS V°), for (Water, TiO_2 0.2% & Al_2O_3 0.2%).

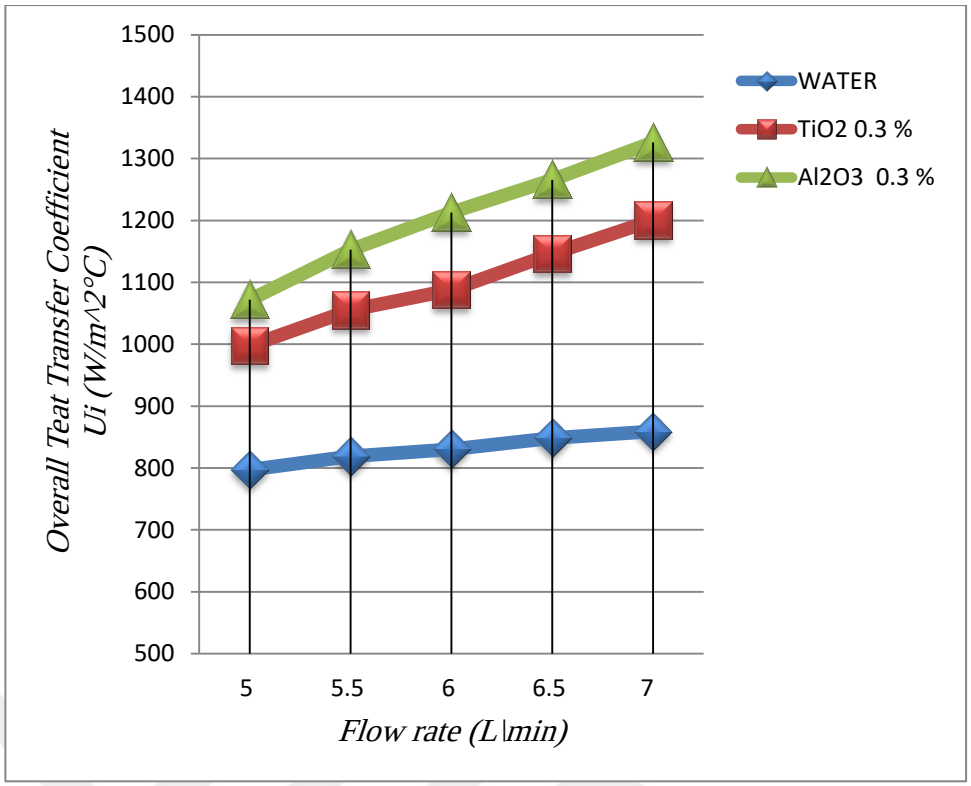

Figure (4.11): The graph of (Ui VS V° **),** for (Water, TiO_2 0.3% & Al_2O_3 0.3%).

The overall heat transfer coefficients of the water and nanofluids of Al_2O_3\water in concentrations of (0.1, 0.2 and 0.3%) in given flow rates of 5, 5.5, 6, 6.5 and 7 L\m were compared as in figure (4.12), and The overall heat transfer coefficients of water and nanofluids of TiO_2\water in concentrations of (0.1, 0.2 and 0.3%) were compared as in figure (4.13), for given flow rates of 5, 5.5, 6, 6.5 and 7 L\m, too.

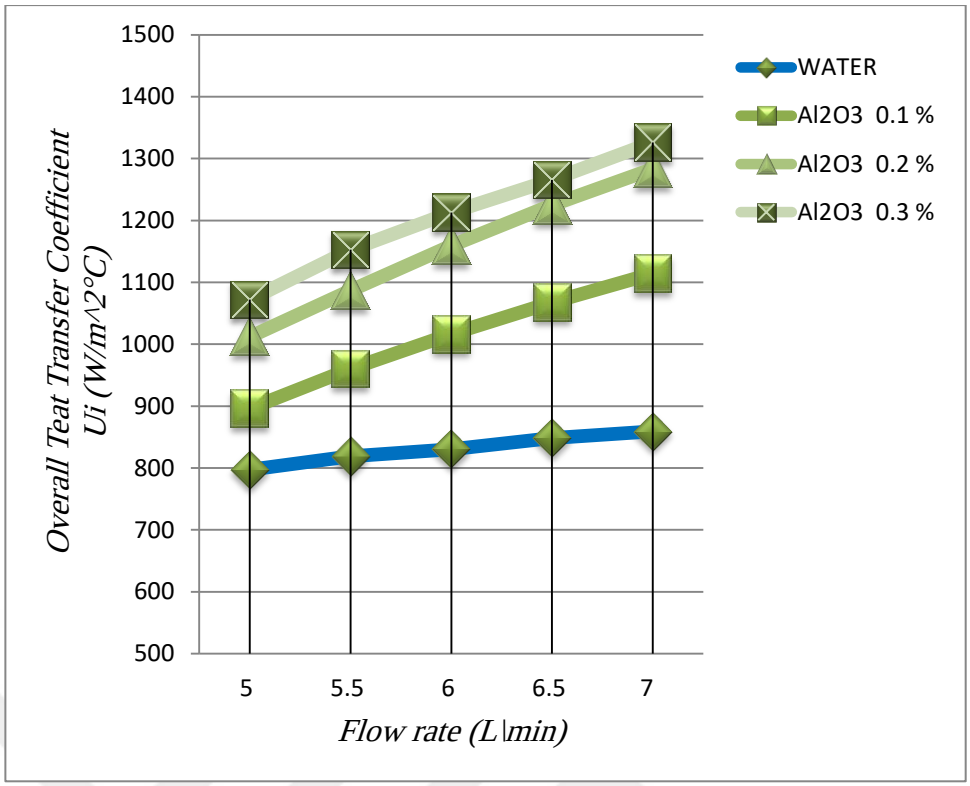

Figure (4.12): The graph of (Ui VS V°), for (Water & Al_2O_3 0.1, 0.2 & 0.3%).

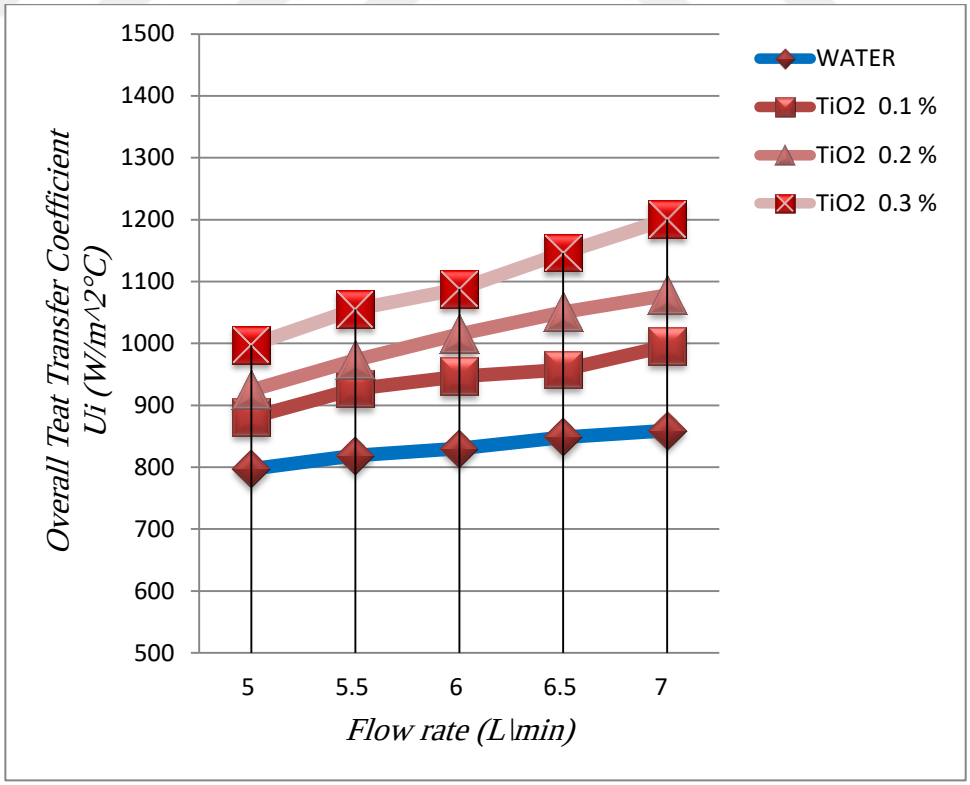

Figure (4.13): The graph of (Ui VS V°), for (Water & TiO_2 0.1, 0.2 & 0.3%).

Figures (4.9, 10, 11, 12 & 13) showed that the enhancement of overall heat transfer coefficient is directly proportional to the increase in concentration of nanofluids, and its value in nanofluids is higher than its value in the water. Farther more, the value of the overall heat transfer coefficient in Al_2O_3\water nanofluids is higher than TiO_2\water nanofluid and water respectively. In addition, it is directly proportional to the increase of flow rate.

4.4.3 Heat transfer coefficient versus flow rate

The comparison of the value of heat transfer coefficient among water, Al_2O_3\water nanofluids and TiO_2\water nanofluids is shown in Figures (4.14), (4.15) and (4.16) for concentrations of 0.1, 0.2 and 0.3% for nanofluids, respectively.

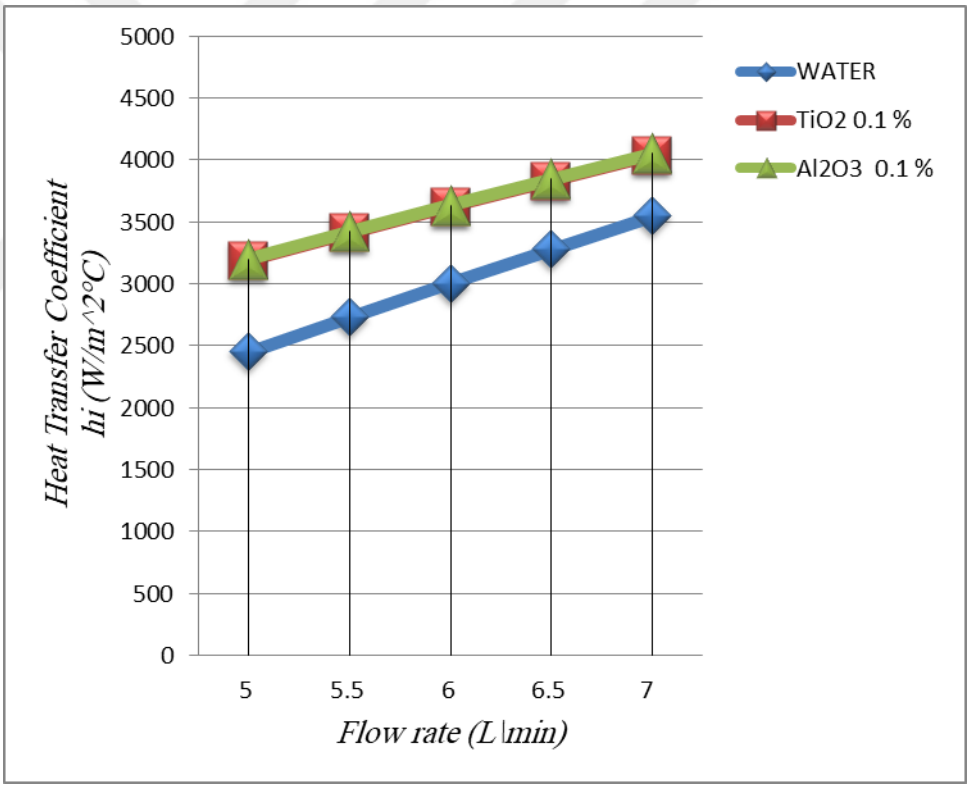

Figure (4.14): The graph for (hi VS V°), for (Water, TiO_2 0.1% & Al_2O_3 0.1%).

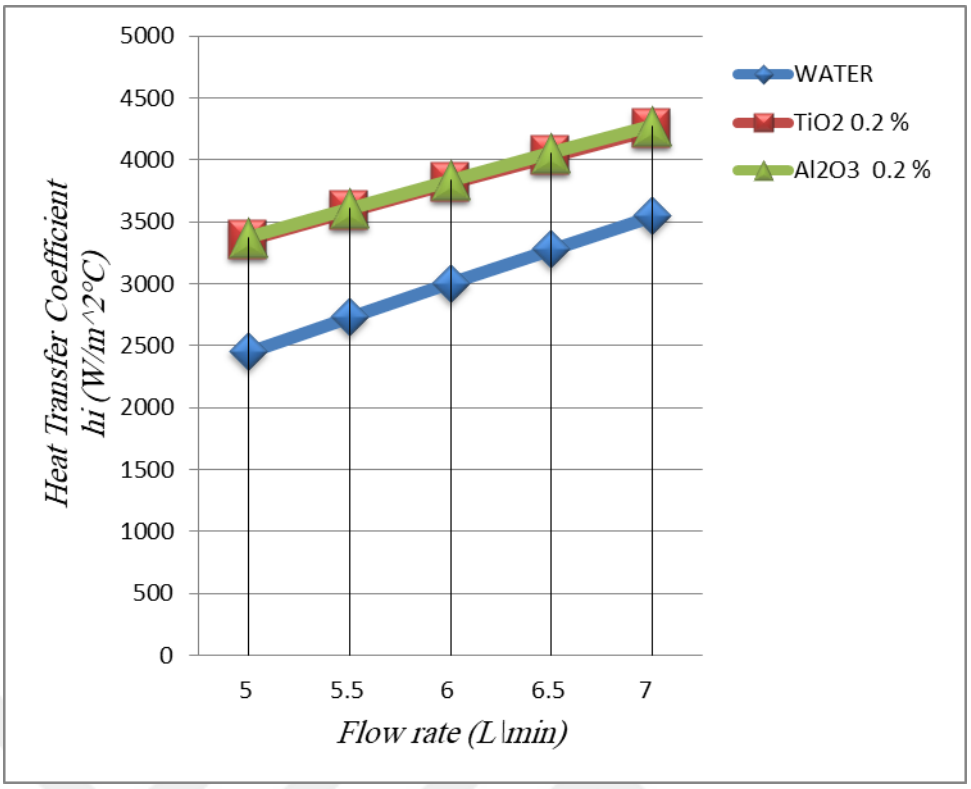

Figure (4.15): The graph for (hi VS V°), for (Water, TiO_2 0.2% & Al_2O_3 0.2%).

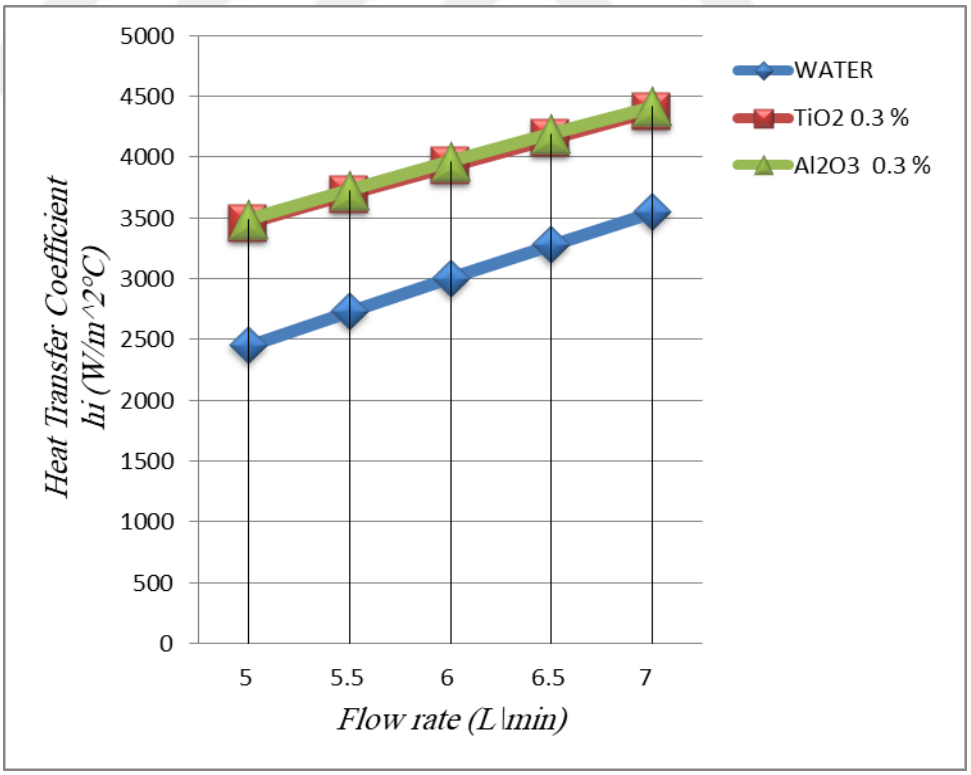

Figure (4.16): The graph for (hi VS V°), for (Water, TiO_2 0.3% & Al_2O_3 0.3%).

The comparison of the value of heat transfer coefficient among water and Al_2O_3\water nanofluids in concentrations of 0.1, 0.2 and 0.3% is shown in figure (4.17).

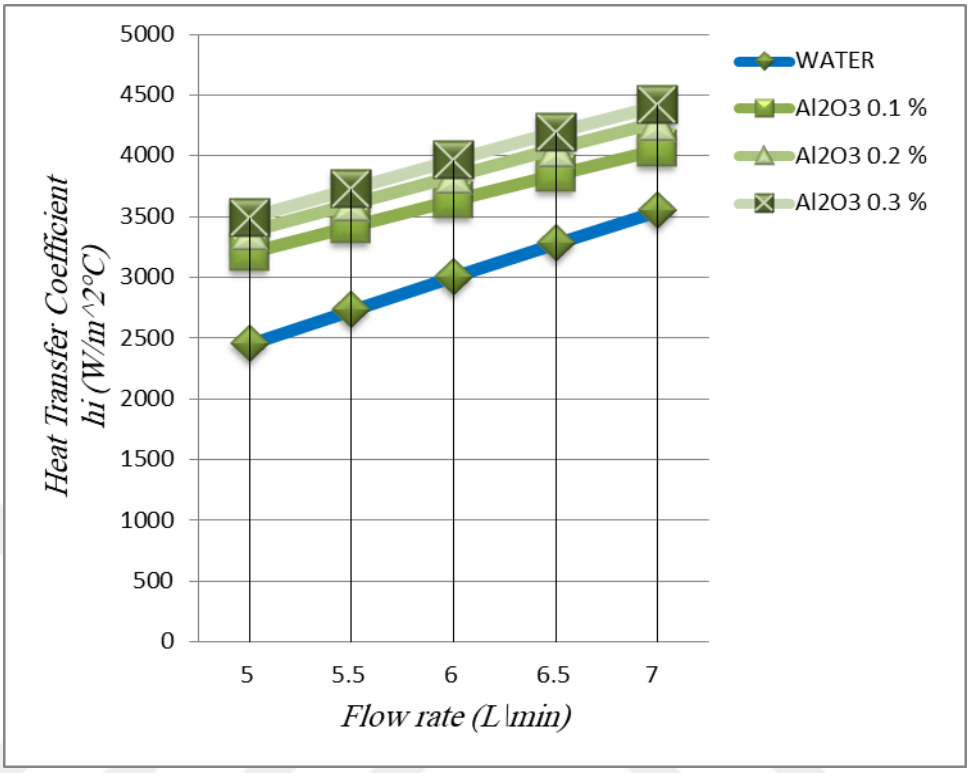

Figure (4.17): The graph for (hi VS V°), for (Water, Al2O3 0.1, 0.2 & 0.3%).

The comparison of the value of heat transfer coefficient among water and TiO_2\water nanofluids in concentrations of 0.1, 0.2 and 0.3% is shown in figure (4.18).

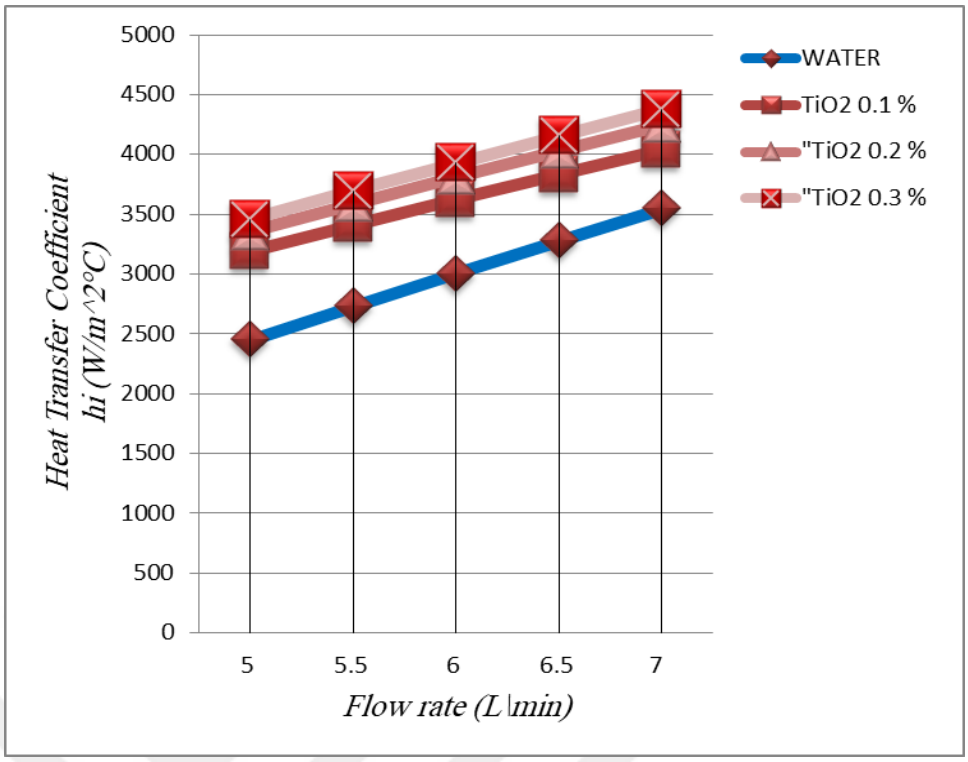

Figure (4.18): The graph for (hi VS V°), for (Water & TiO_2 0.1, 0.2 & 0.3%).

From the figures (4.14), (4. 15), (4.16), (4.17) and (4.18), it was cleared that heat transfer coefficient of the nanofluid is greater than heat transfer coefficient of distilled water. For the nanofluids, the amount of the heat transfer coefficient increased directly with increasing of particle volume concentration of nanofluid. Farther more, the heat transfer coefficient in a given concentration for Al_2O_3\water nanofluid is greater than heat transfer coefficient of TiO_2\water nanofluid in same concentration value, and the best value of heat transfer coefficient was recorded in a concentration of 0.3% of Al_2O_3\water nanofluid.

4.4.4 Nusselt number versus flow rate

Figures (4.19), (4.20) and (4.21) showed Nusselt number enhancement ratio, which is the ratio of TiO_2\water and Al_2O_3\water nanofluids to Nusselt number of pure water, for different nanoparticles concentrations of 0.1, 0.2 and 0.3%, in various mass flow rate of 5, 5.5, 6, 6.5 and 7 L\m. It was clear that the addition of nanoparticles to the base fluid increased the value of Nusselt number for both kinds of nanofluids, and it is a little bit better in TiO_2\water than Al_2O_3\water because of the difference in viscosity for each of them.

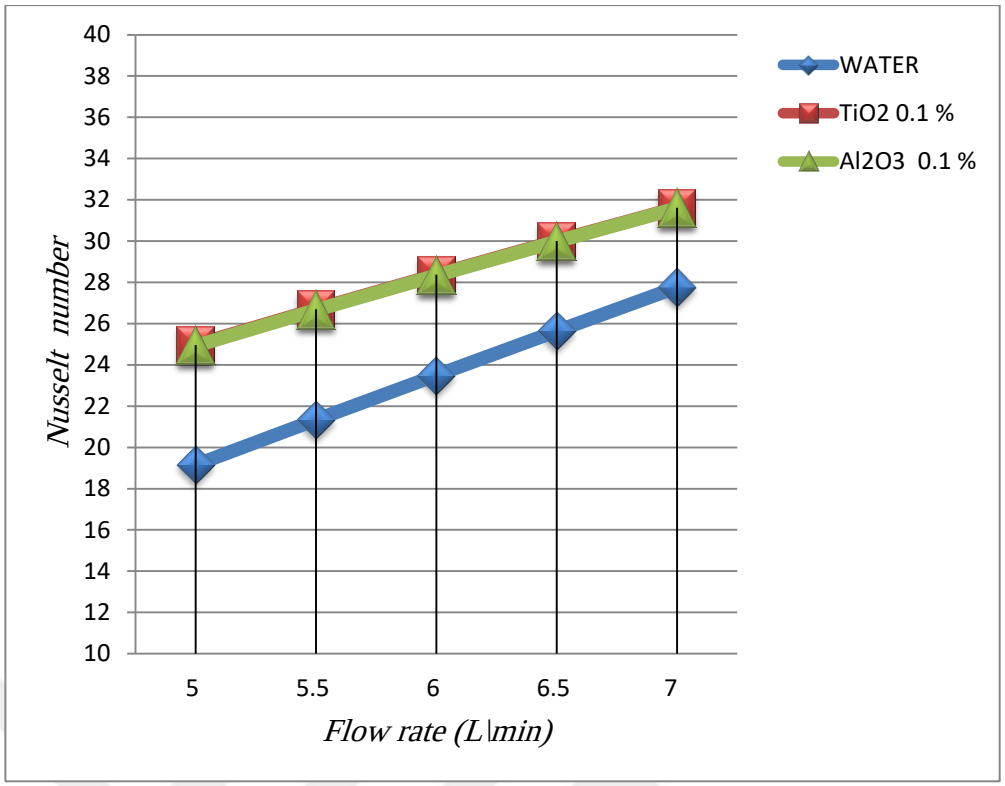

Figure (4.19): The graph for (Nu VS V°), for (Water, TiO_2 0.1% & Al_2O_3 0.1%).

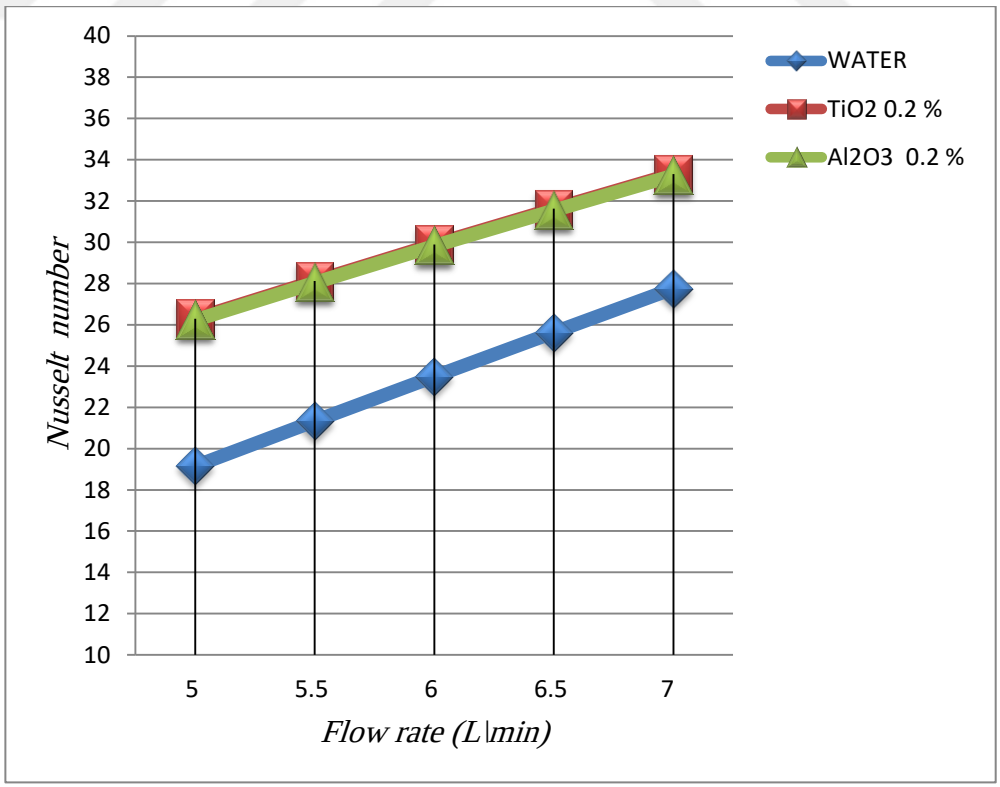

Figure (4.20): The graph for (Nu VS V°), for (Water, TiO_2 0.2% & Al_2O_3 0.2%).

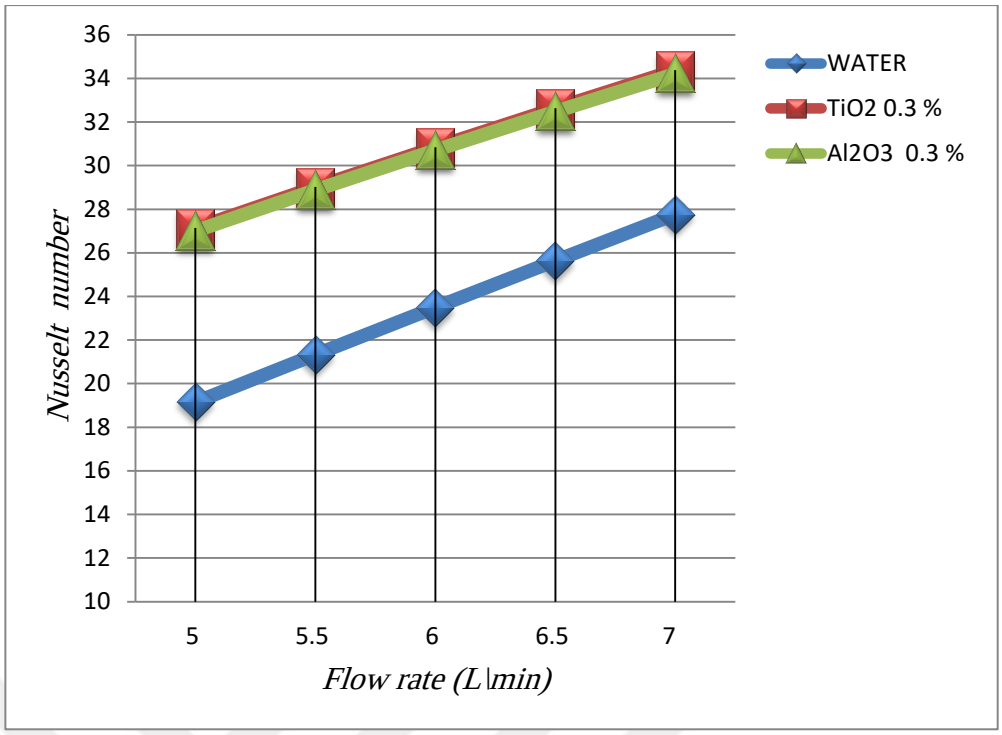

Figure (4.21): The graph for (Nu VS V°), for (Water, TiO_2 0.3% & Al_2O_3 0.3%).

Figure (4.22) represents a comparison of Nusselt number for water and TiO_2\water in concentrations of 0.1, 0.2 and 0.3% versus a given mass flow rates of 5, 5.5, 6, 6.5 and 7 L\m.

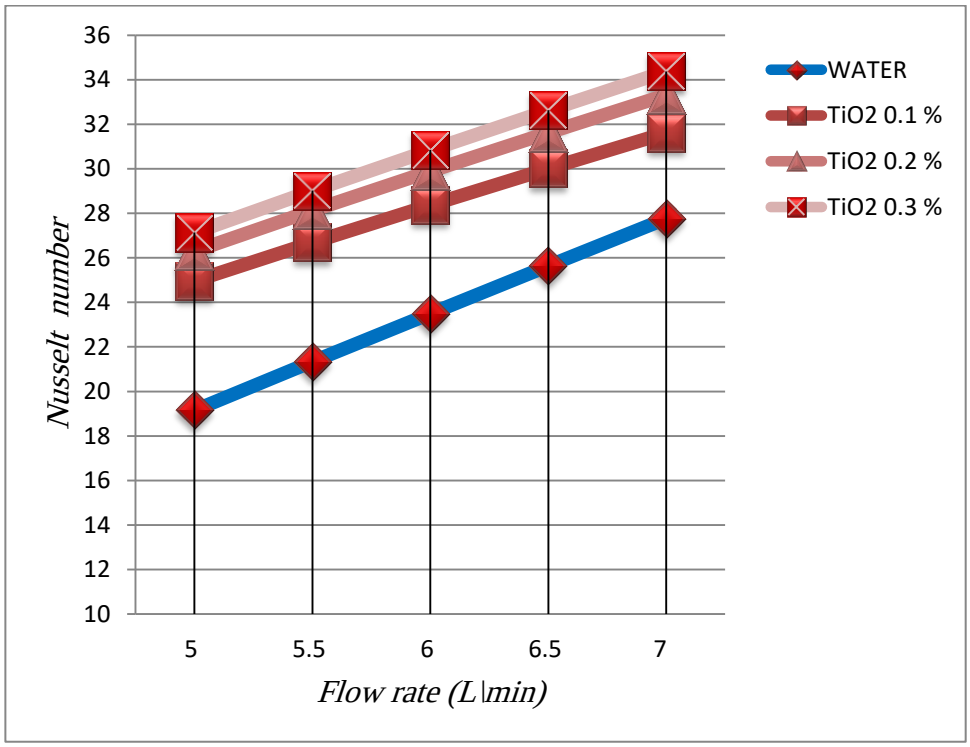

Figure (4.22): The graph for (Nu VS V°), for (Water & TiO_2 0.1, 0.2 & 0.3%).

In addition, Figure (4.23) represents a comparison of Nusselt number for water and Al_2O_3\water in concentrations of 0.1, 0.2 and 0.3% versus a given mass flow rates of 5, 5.5, 6, 6.5 and 7 L\m.

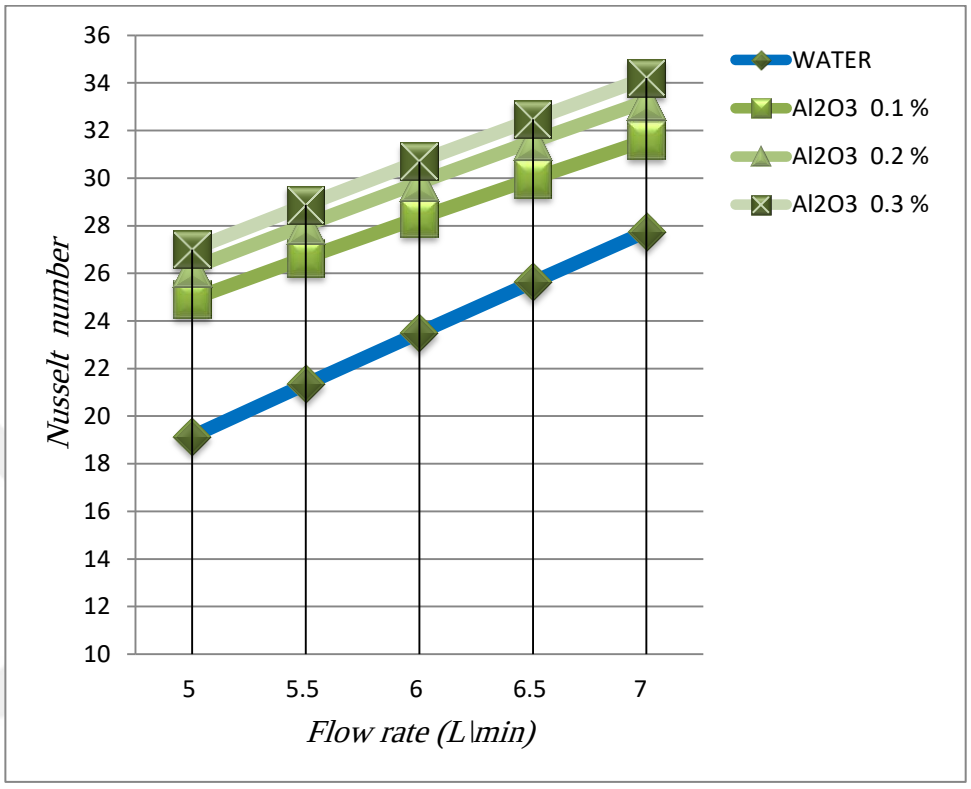

Figure (4.23): The graph for (Nu VS V°), for (Water & Al_2O_3 0.1, 0.2 & 0.3%).

As expected from the last five figures, Nusselt number increased with increasing the mass flow rate, and it is increasing with increasing of the concentration of the nanofluids. In addition, Nusselt number in Al_2O_3\water is greater than Nusselt number of TiO_2\water, and the highest value is in a concentration of 0.3% of Al_2O_3\water nanofluid.

4.4.5 Reynolds number versus flow rate

For the determination of the relationships for Reynolds number versus mass flow rates of 5, 5.5, 6, 6.5 and 7 L\m for water and nanofluids of Al_2O_3\water and TiO_2\water in concentrations of 0.1, 0.2 &0.3% for each of them, figures (4.24),

(4.25) and (4.26) were evident that Reynolds number was higher in nanofluids than water. Moreover, it increased a little with increasing concentration of nanofluids according to the variable value in viscosities because of the effect of adding nano particle

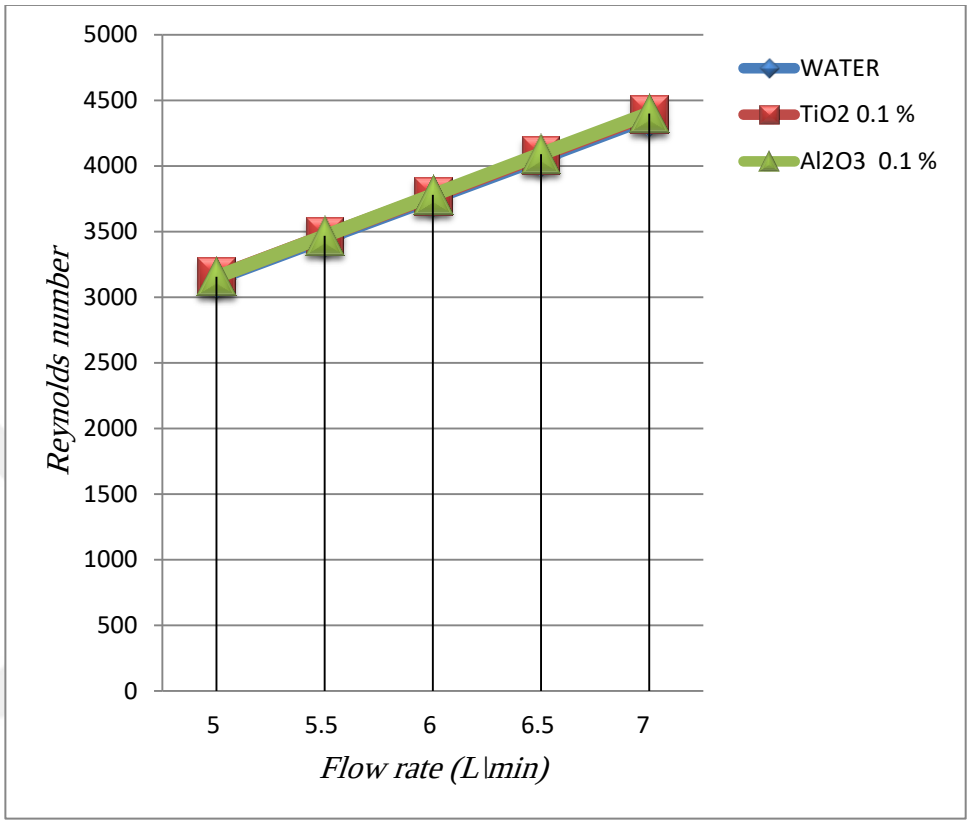

Figure (4.24): The graph of (Re VS V°), for (Water, TiO_2 0.1% & Al_2O_3 0.1%).

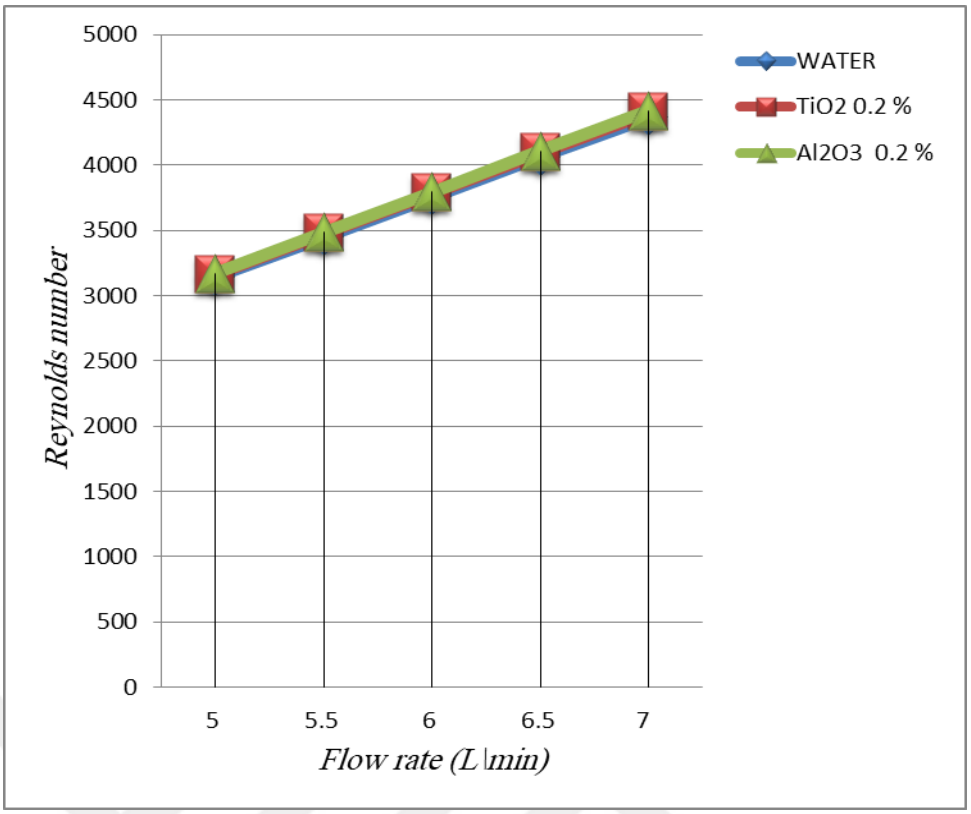

Figure (4.25): The graph of (Re VS V°), for (Water, TiO_2 0.2% & Al_2O_3 0.2%).

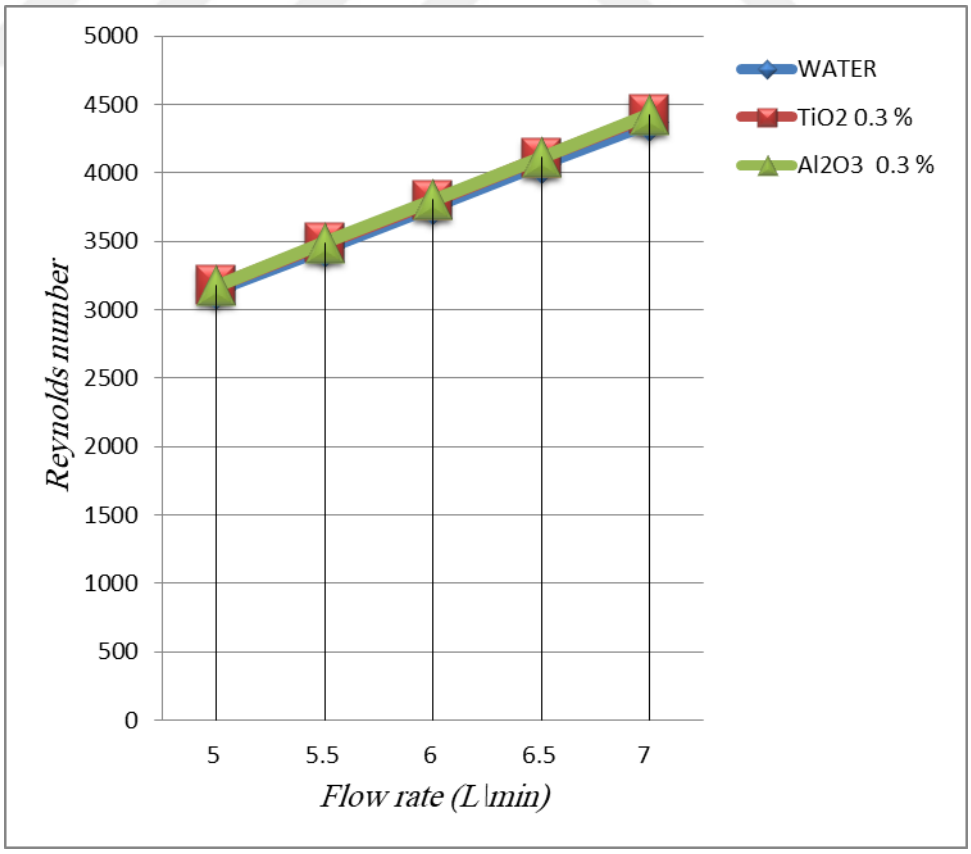

Figure (4.26): The graph of (Re VS V°), for (Water, TiO_2 0.3% & Al_2O_3 0.3%).

TiO_2 nanoparticles in water with concentrations of 0.1, 0.2%, and 0.3% were compared with pure water for the value of Reynolds number in a difference flow rates of 5, 5.5, 6, 6.5 and 7L\m, as shown in Figure (4.27). Moreover, Al_2O_3 nanoparticles in water with concentrations of 0.1, 0.2%, and 0.3% were compared with pure water for the value of Reynolds number in a difference flow rates of 5, 5.5, 6, 6.5 and 7L\m, as shown in figure (4.28). From the figures (4.29) and (4.30), it was concluded that Reynolds number increased by increasing the concentration of nanofluid, and it is higher in Al_2O_3 \water than TiO_2 \water and water, respectively. The maximum value of Reynolds number was observed at the highest concentration of Al_2O_3 \water nanofluid of 0.3%.

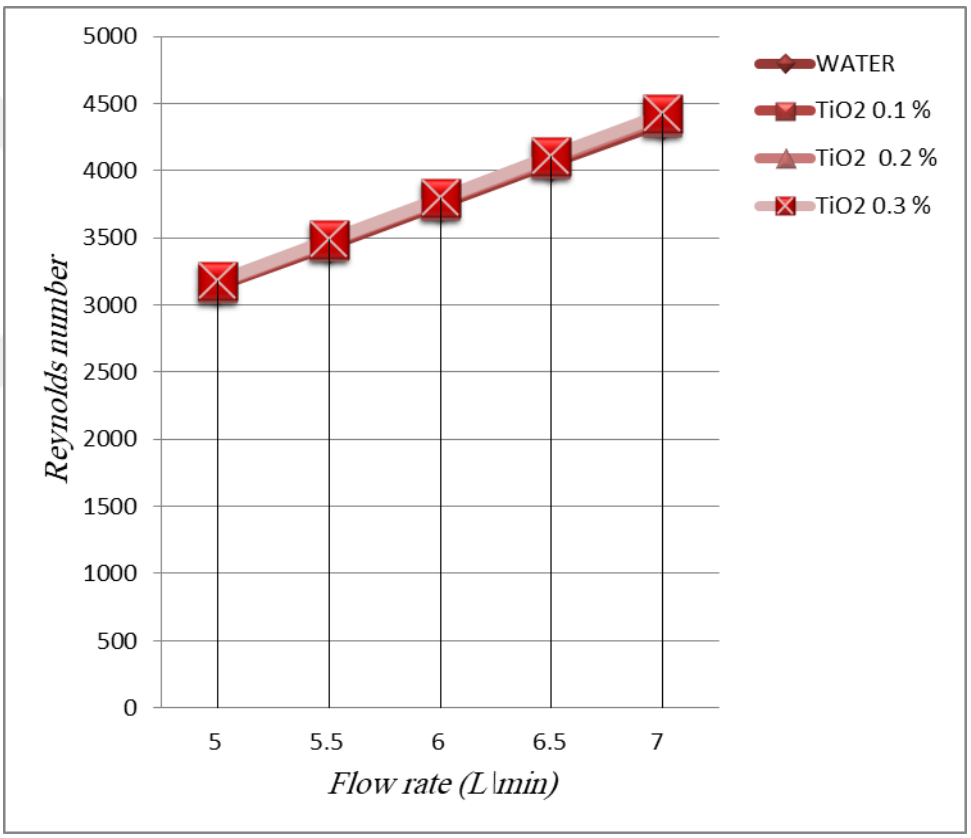

Figure (4.27): The graph of (Re VS V°), for (Water, TiO_2 0.1, 0.2 & 0.3%).

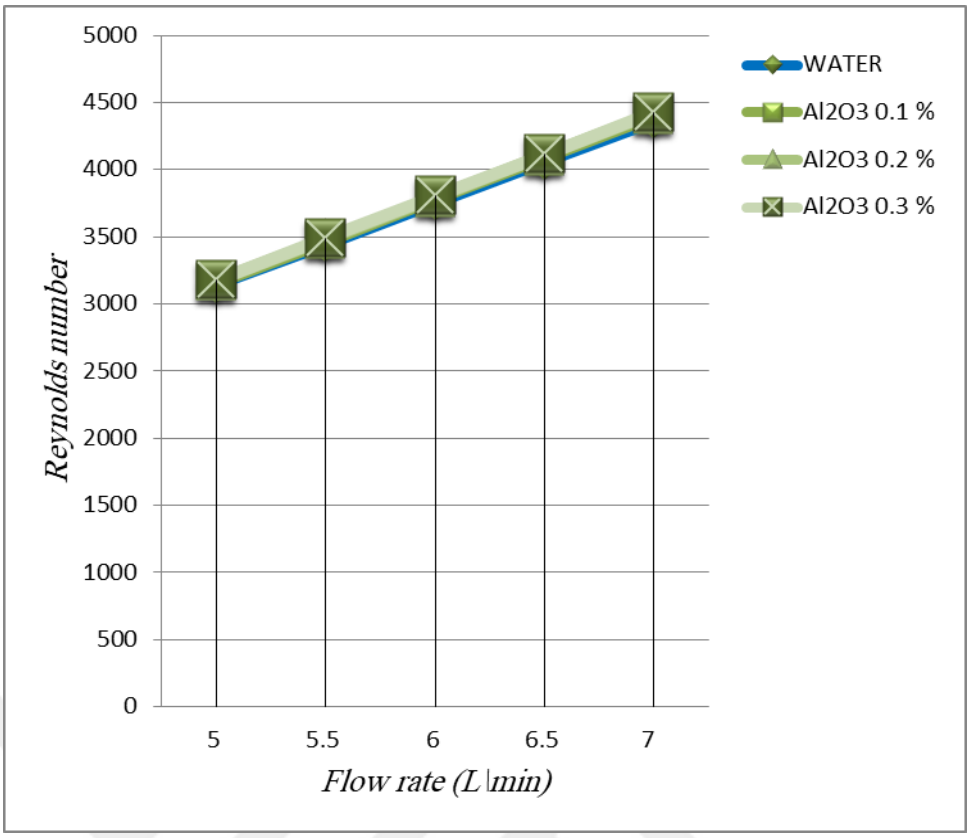

Figure (4.28): The graph of (Re VS V°), for (Water, Al_2O_3 0.1, 0.2 & 0.3%).

4.4.6 Reynolds number versus Nusselt number

Figure (4.29) shows the variation of Nusselt number with (Re) of base fluid according to mass flow rates of 5, 5.5, 6, 6.5 and 7L\m. As can be seen from this figure, Nusselt number increases remarkably with increasing Reynolds number in each value of flow rates.

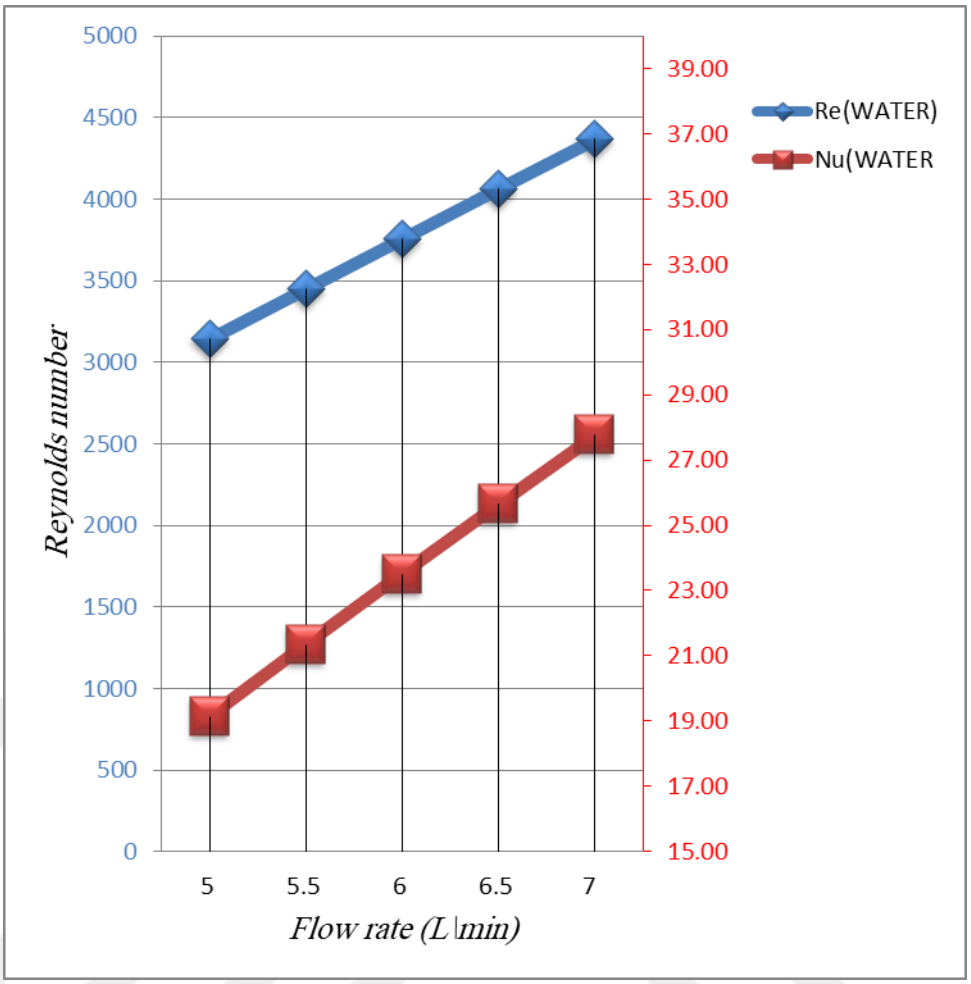

Figure (4.29): The relation of (Re VS Nu) for water, (according to given volume flow rate).

Figures (4.30), (4.31) and (4.32) showed the variation of Nusselt number with Reynolds number of TiO_2\water in concentrations of 0.1, 0.2 &0.3% respectively, and according to mass flow rates of 5, 5.5, 6, 6.5 and 7L\m. These figures declared that Nusselt number increases with increasing Reynolds number in each concentration value. Even more, the increasing ratio of Nusselt number is higher than increasing ratio of Reynolds number for each concentration according to the given mass flow rates.

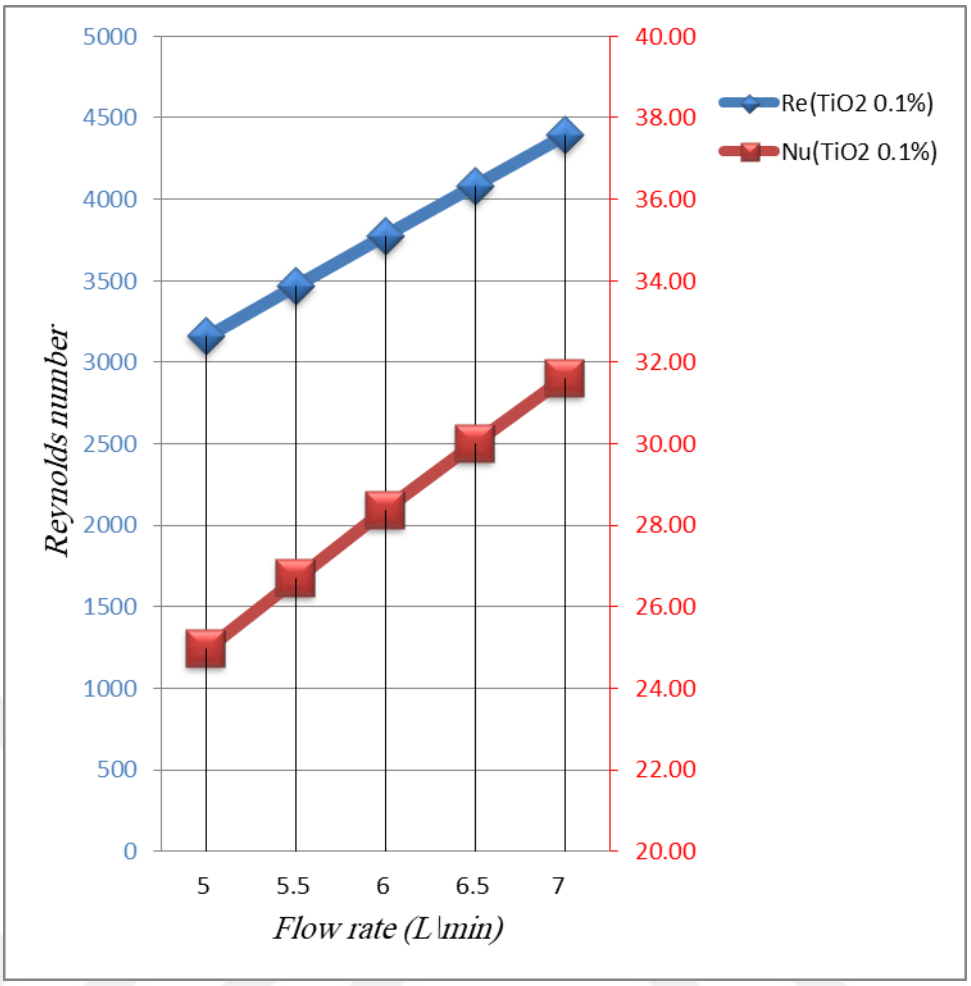

Figure (4.30): The relation of (Re VS Nu) for TiO_2\water 0.1 %, (according to given volume flow rate).

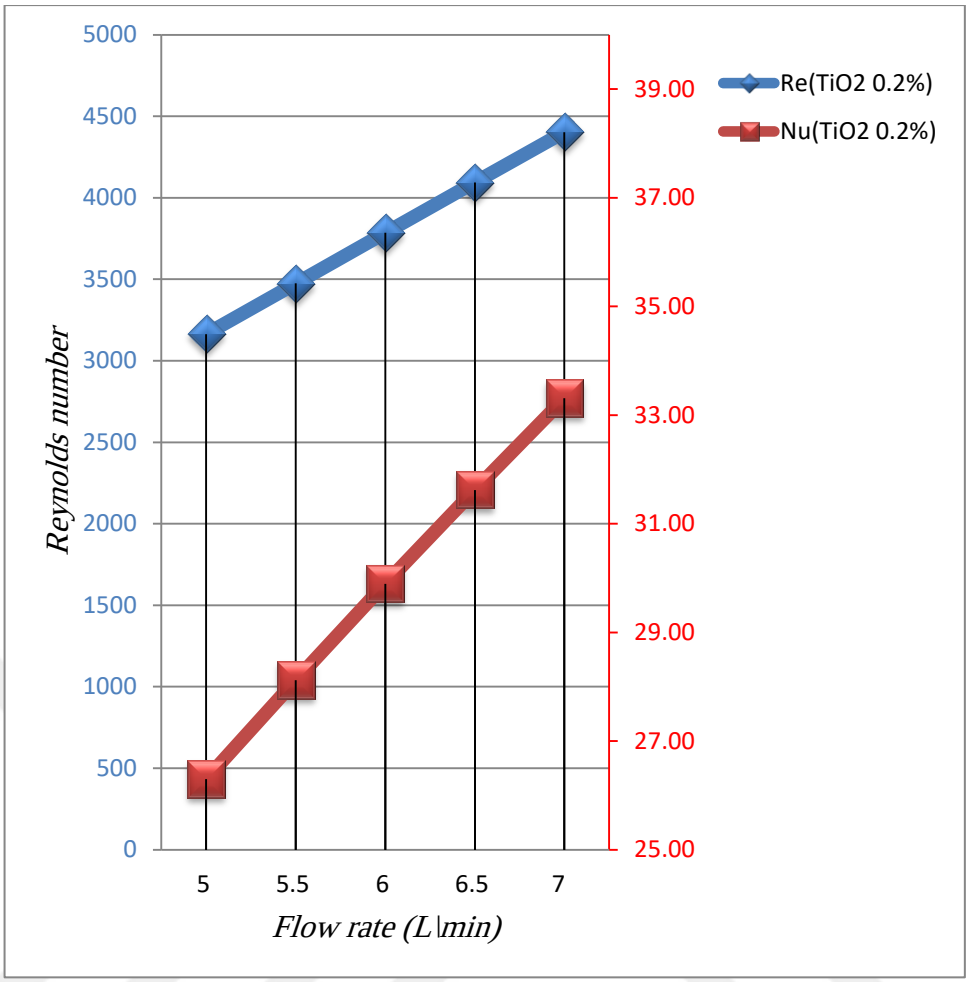

Figure (4.31): The relation of (Re VS Nu) for TiO_2\water 0.2 %, (according to given volume flow rate).

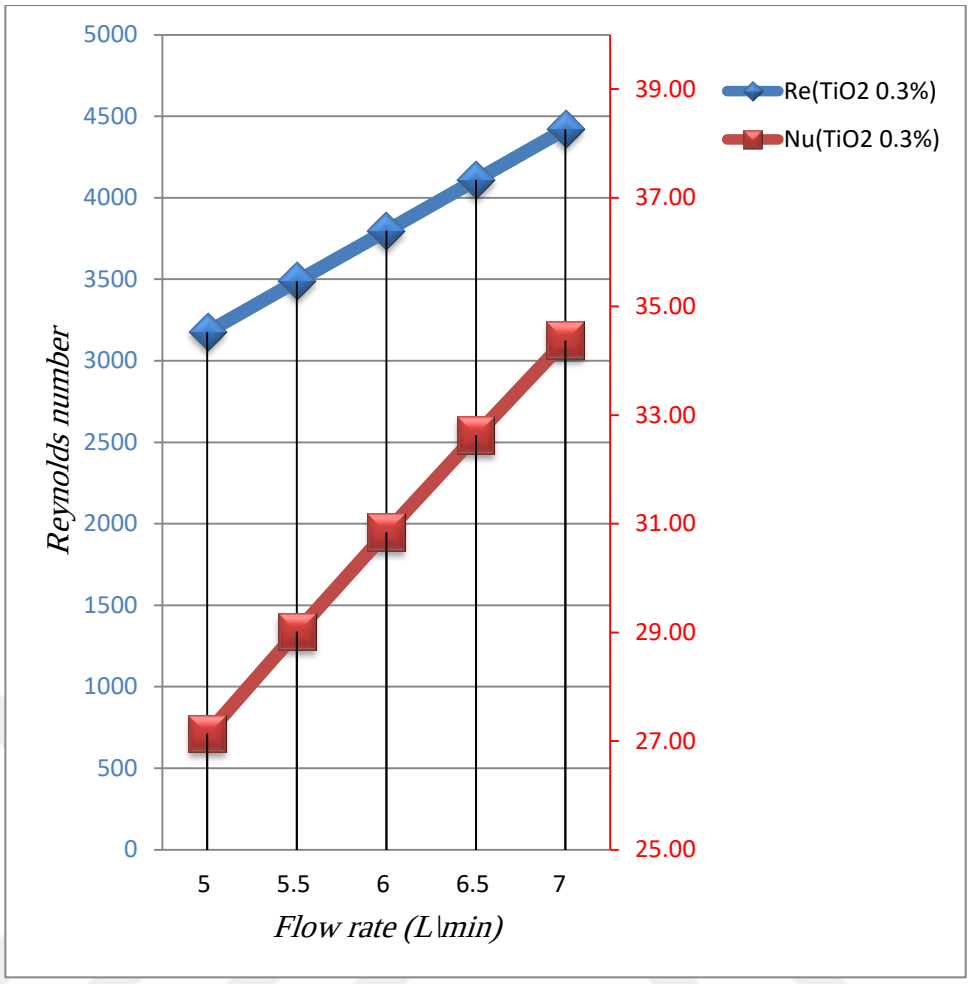

Figure (4.32): The relation of (Re VS Nu) for TiO_2\water 0.3 %, (according to given volume flow rate).

The variation of Nusselt number with Reynolds number of Al_2O_3\water in concentrations of 0.1, 0.2 &0.3% according to flow rates of 5, 5.5, 6, 6.5 and 7L\m were shown in figures (4.33), (4.34) and (4.35) respectively. These figures declared that Nusselt number increases with increasing of Reynolds number in each concentration value. Even more, the increasing ratio of Nusselt number is higher than increasing ratio of Reynolds number for each concentration according to the given mass flow rates.

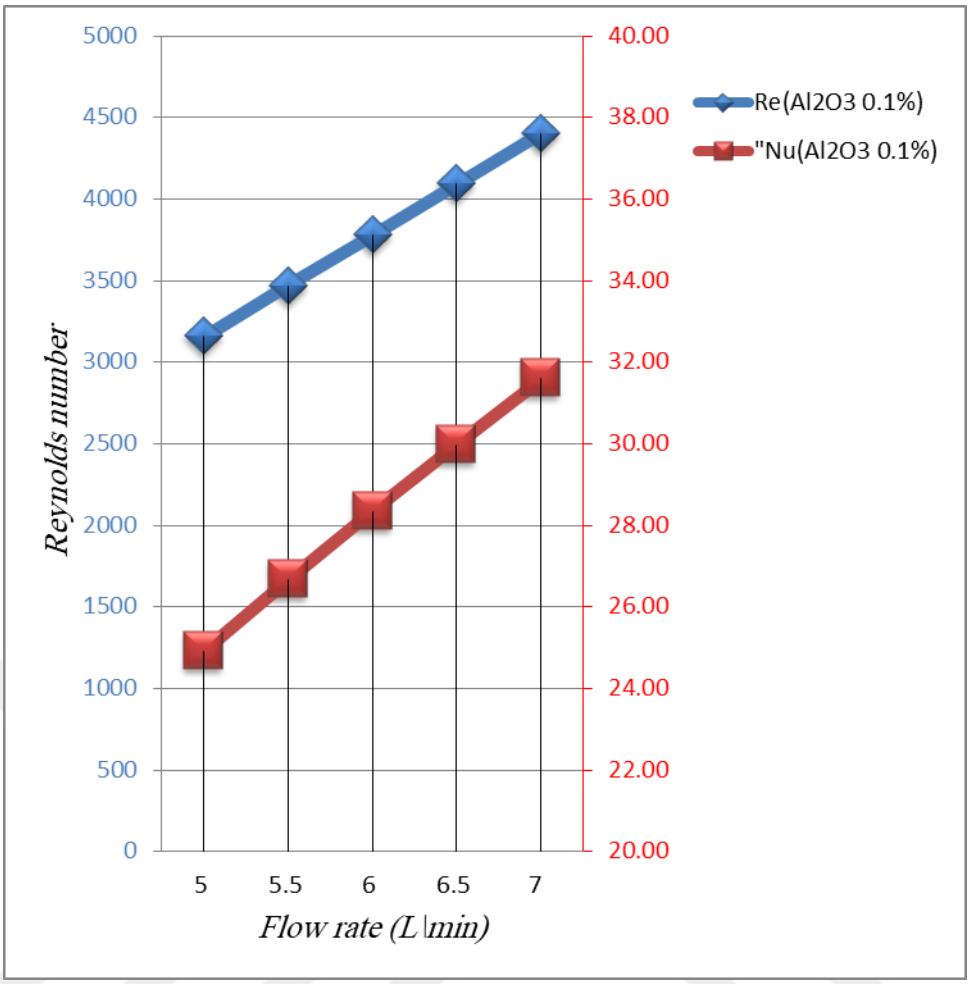

Figure (4.33): The relation of (Re VS Nu) for Al_2O_3\water 0.1%, (according to given volume flow rate).

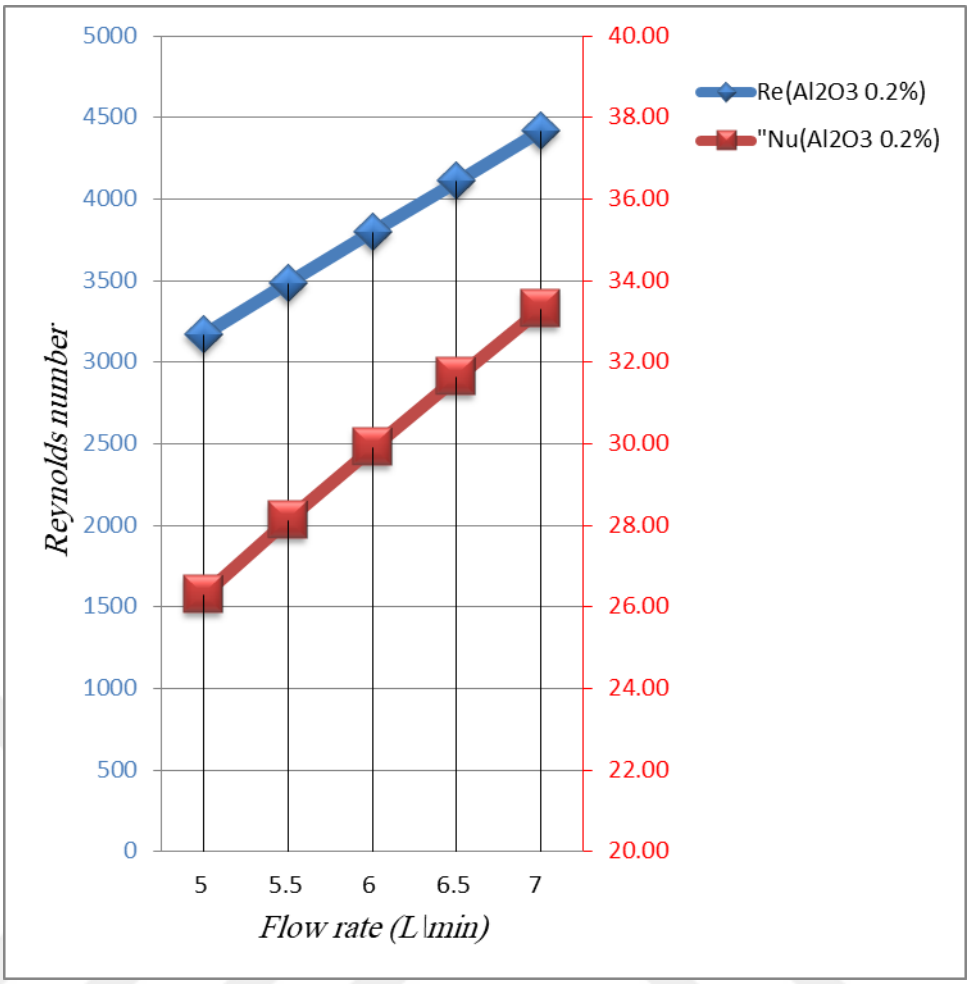

Figure (4.34): The relation of (Re VS Nu) for Al_2O_3\water 0.2%, (according to given volume flow rate).

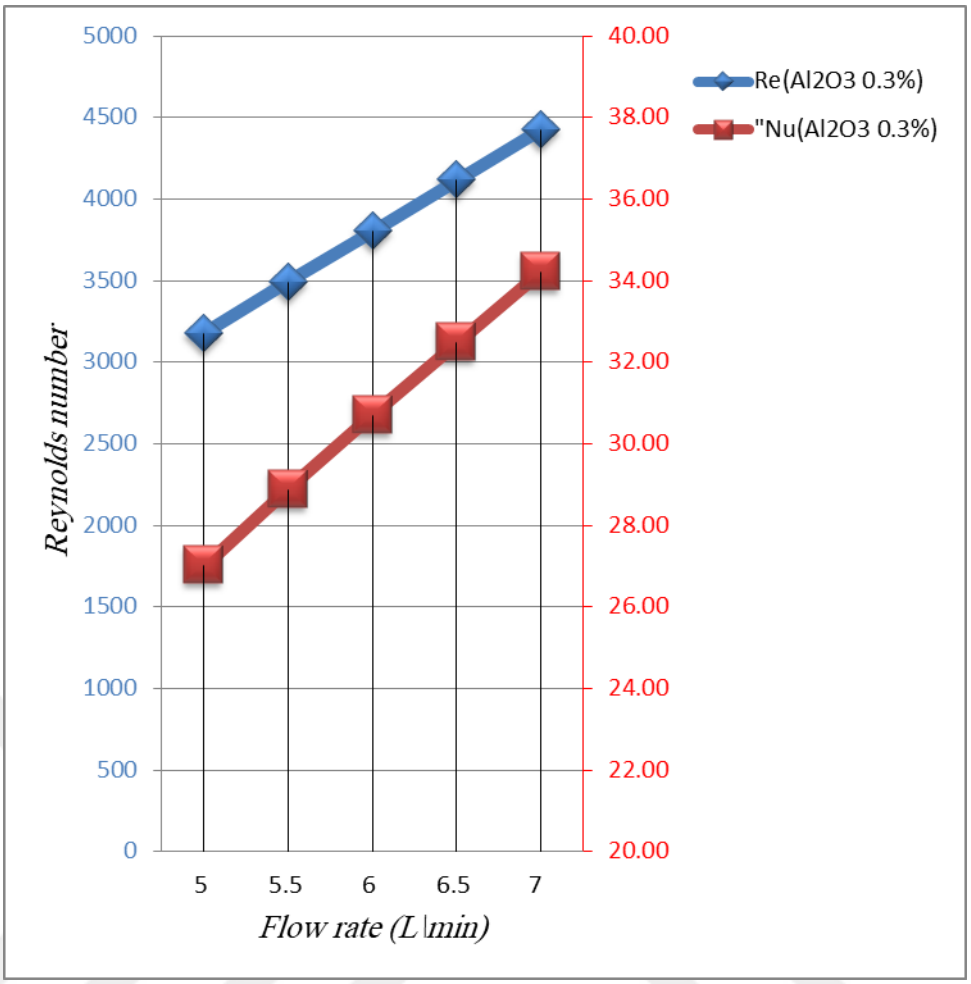

Figure (4.35): The relation of (Re VS Nu) for Al_2O_3\water 0.3%, (according to given volume flow rate).

4.4.7 Overall heat transfer coefficient versus Nusselt number

To declare the relations between overall heat transfer coefficient and Nusselt number, Figures (4.36), (4.37), (4.38), (4.39), (4.40), (4.41) and (4.42) showed these relations for the water and for the nanofluids of Al_2O_3\water and TiO_2\water in three concentrations of 0.1, 0.2 and 0.3% for each of them.

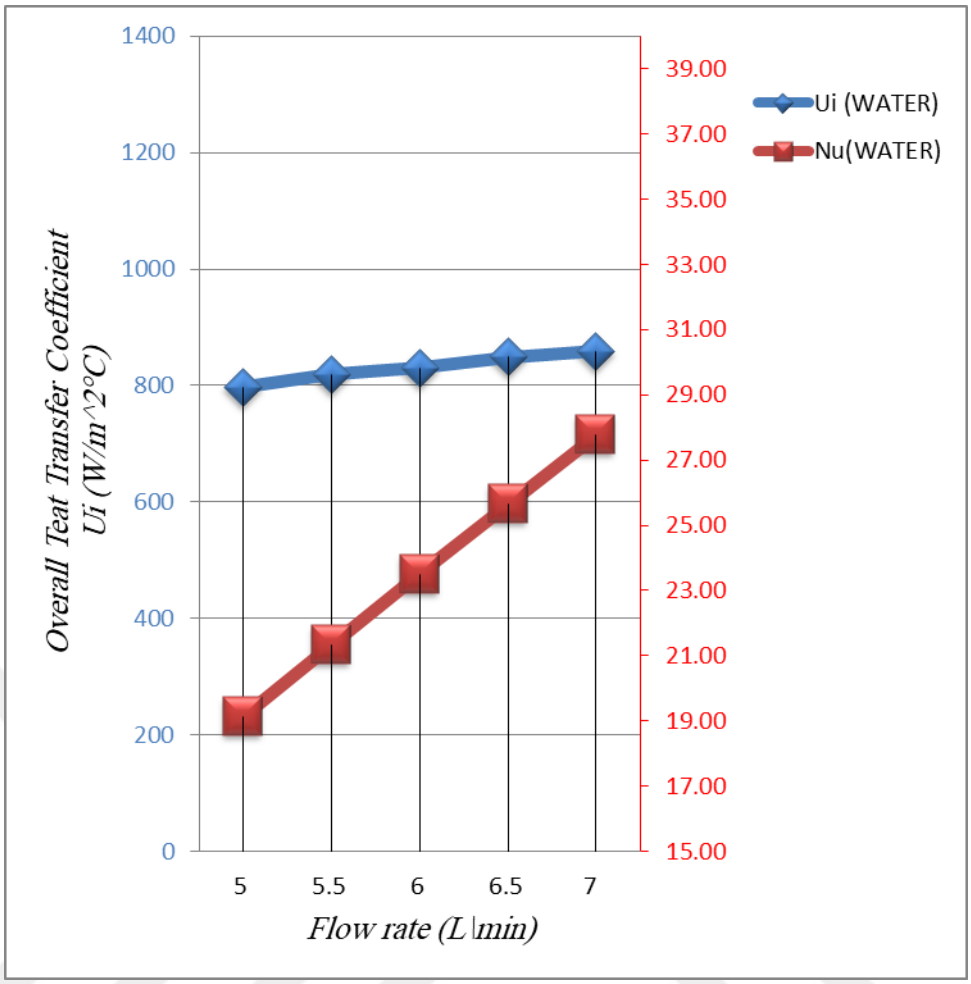

Figure (4.36): The relation of (Ui VS Re) for water, (according to given volume flow rate).

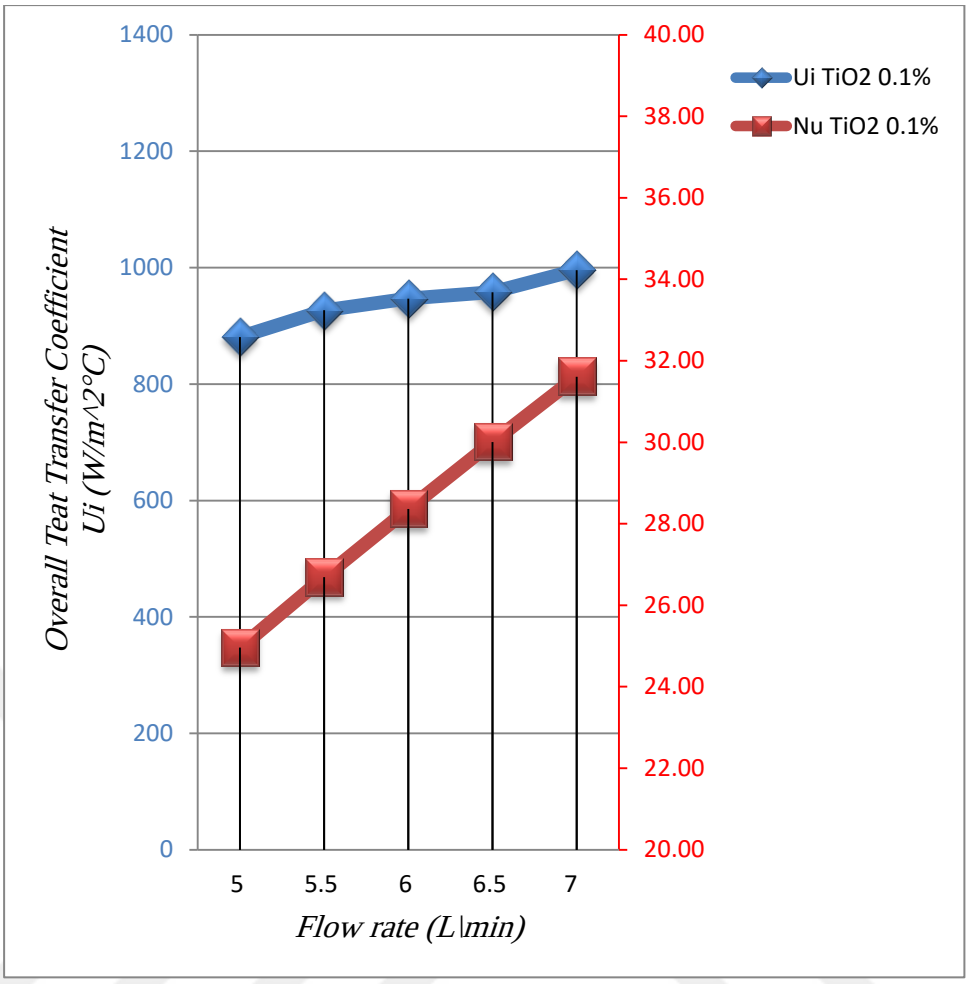

Figure (4.37): The relation of (Ui VS Re) for TiO_2 0.1 %, (according to given volume flow rate).

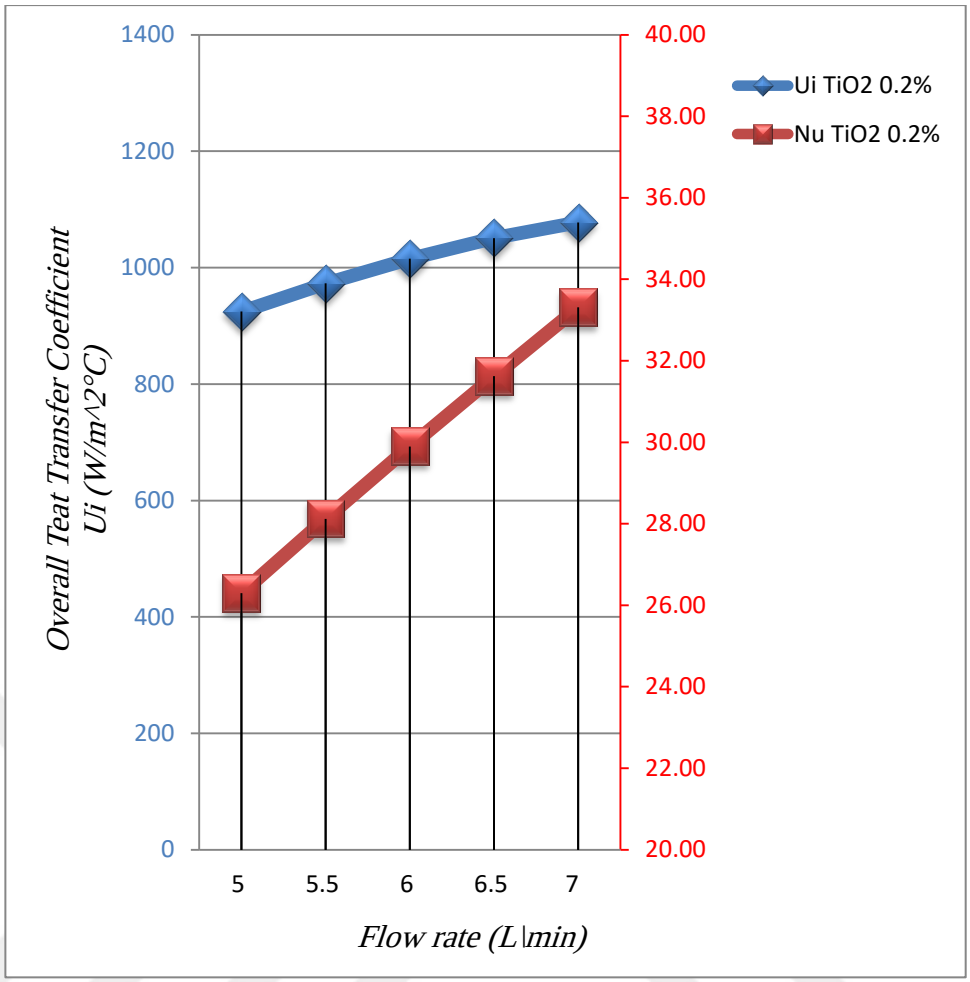

Figure (4.38): The relation of (Ui VS Re) for TiO_2 0.2 %, (according to given volume flow rate).

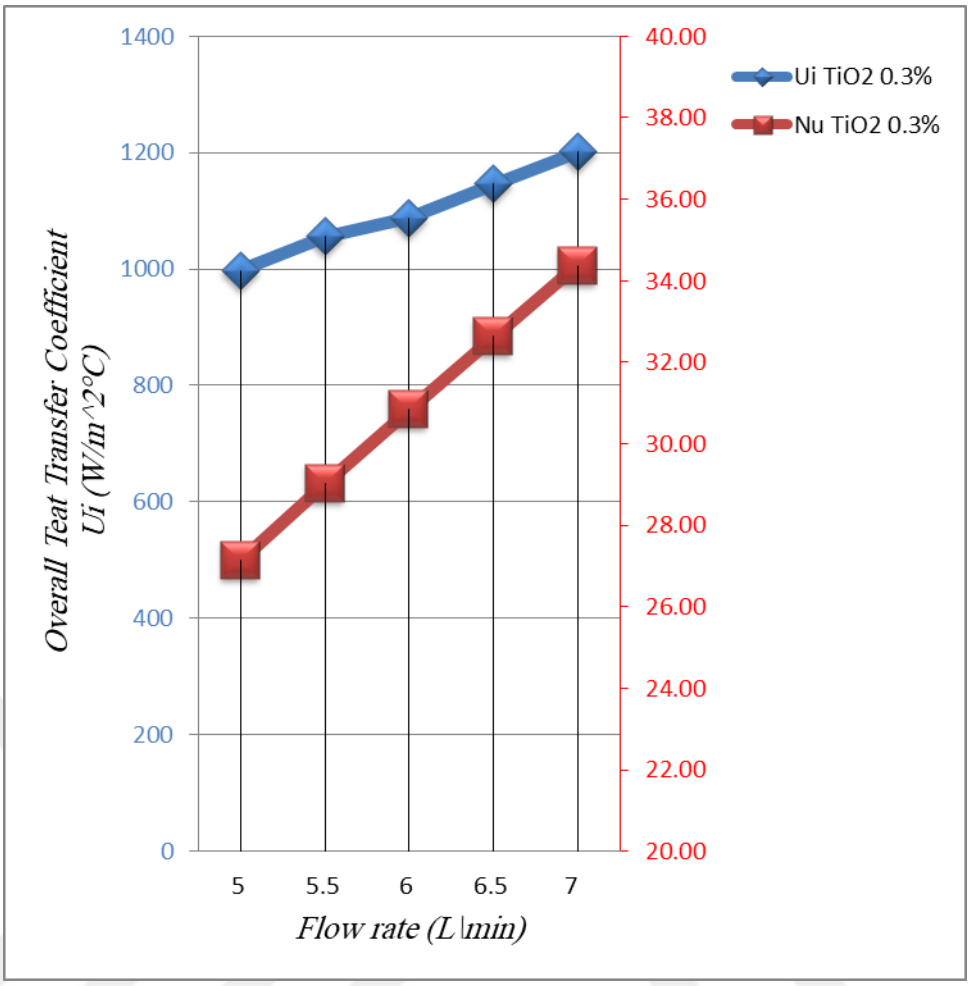

Figure (4.39): The relation of (Ui VS Re) for TiO_2 0.3 %, (according to given volume flow rate).

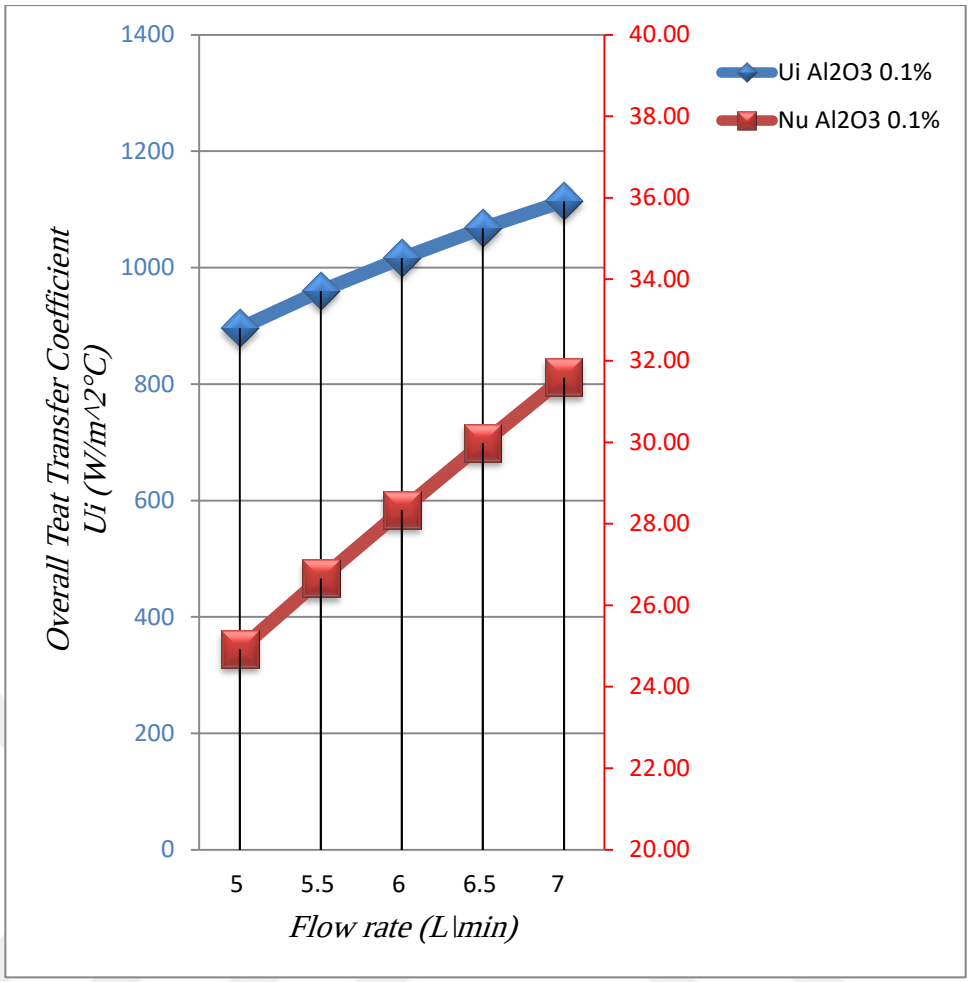

Figure (4.40): The relation of (Ui VS Re) for Al_2O_3 0.1 %, (according to given volume flow rate).

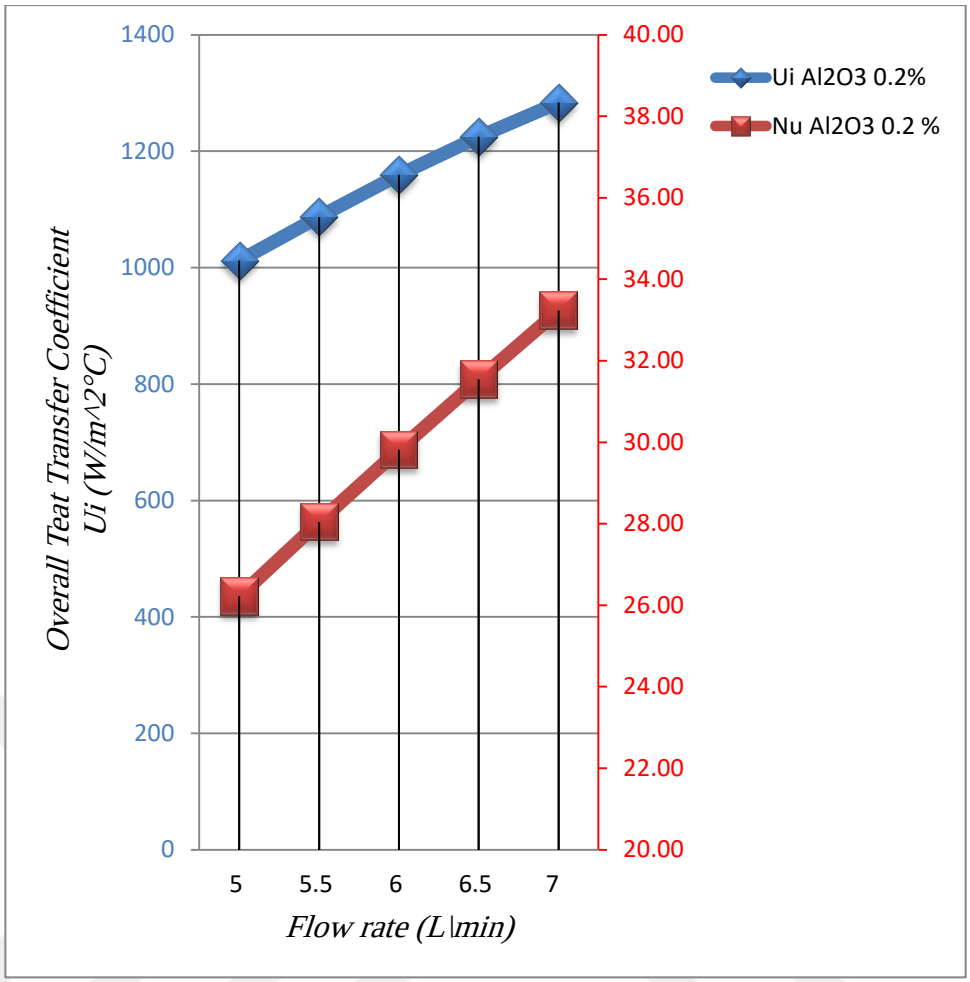

Figure (4.41): The relation of (Ui VS Re) for Al_2O_3 0.2 %, (according to given volume flow rate).

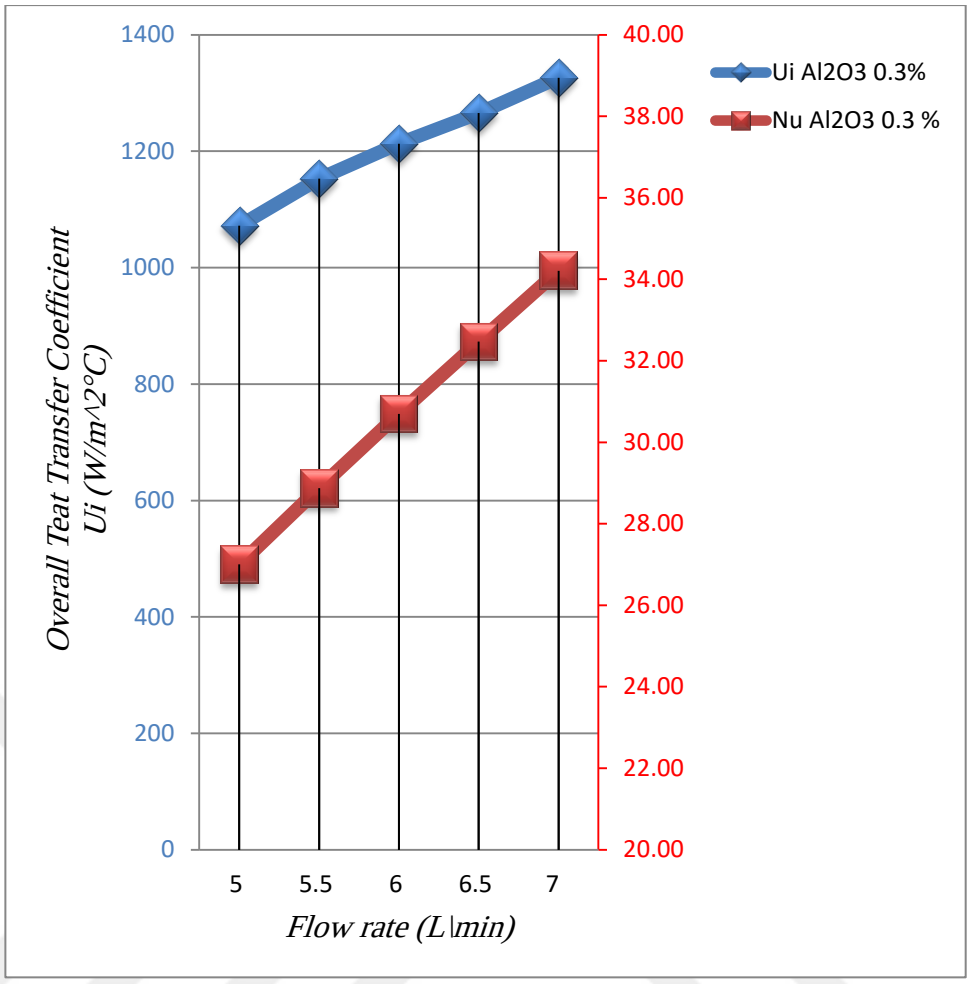

Figure (4.42): The relation of (Ui VS Re) for Al_2O_3 0.3 %, (according to given volume flow rate).

The results, which presented in the seven previews figures, showed that the overall heat transfer coefficient increases with increasing of Nusselt number. Furthermore, the effect of adding nanoparticles caused increasing in both of overall heat transfer coefficient and Nusselt number, but the ratio of the difference between the maximum and minimum value of overall heat transfer coefficient to the difference between the maximum and minimum value of Nusselt number for the one kind of nanofluids in given five flow rates was increased directly with increasing of the concentration of the nanofluid. It is mean that the increase in Nusselt number ratio was more than that in overall heat transfer coefficient.

CHAPTER FIVE

CONCLUSION AND FUTURE WORK

5.1 Conclusion

In the present study, it was studied the thermal properties of two types of nanoparticles (Al_2O_3 and TiO_2) which were dissolved in water in volume concentrations of (0.1,0.2 and 0.3 %) for each of them in addition to the base fluid (water) in forced convection heat transfer under turbulent flow and counter flow heat exchanger. Each kind of these fluids was flowed in rates of 5, 5.5, 6, 6.5 and 7 L/m. The main goal of this study is to find the enhancement of the heat transfer rate and the change in values of heat transfer coefficient, overall heat transfer coefficient, Reynolds number and Nusselt number. The parameters that already mentioned were increased with increasing of volume concentration of the nanofluid. In addition, they were higher in Al_2O_3\water than TiO_2\water and water, respectively. On the other hand, these parameters increased with increasing of flow rate except heat transfer coefficient and Nusselt number; they decreased with increasing of flow rate. For these reasons, the highest value of heat transfer coefficient, overall heat transfer coefficient and Reynolds number were in Al_2O_3\water in concentration of 0.3% and flow rate of 7 L\m, and they were higher in Al_2O_3\water nanofluid than TiO_2\water nanofluid "at the same concentration" and water, respectively. Nusselt number and heat transfer coefficient increased with increasing of the volume concentration of nanofluid, and they were higher in Al_2O_3\water than TiO_2\water and water, respectively. But, they were decreased with increasing of flow rate. Nusselt number was higher in TiO_2\water nanofluid than Al_2O_3\water nanofluid and water, respectively. Heat transfer coefficient was higher in Al_2O_3\water nanofluid than TiO_2\water nanofluid and water, respectively. Table (5.1) shows the values of heat transfer rate, overall heat transfer coefficient, heat transfer coefficient, Reynolds number and Nusselt number, as well as it shows the percentage increase for each of them compared to the base fluid (water), for the all experiments.

Table (5.1): The values of the heat transfer rate, overall heat transfer coefficient, heat transfer coefficient, Reynolds number and Nusselt number, and the percentage increase of them compared to base fluid (water).

		TYPE OF NANOFLUID AND ITS CONCENTRATION						THE PERCENTAGE INCREASE IN (%) PROPORTION TO THE WATER					
Flow Rate (m³/s) (L/m	WATER	TiO2 0.1 %	TiO2 0.2 %	TiO2 0.3 %	Al2O3 0.1 %	Al2O3 0.2 %	Al2O3 0.3 %	TiO2 0.1 %	TiO2 0.2 %	TiO2 0.3 %	Al2O3 0.1 %	Al2O3 0.2 %	Al2O3 0.3 %
	Q (W)	Q (W)	Q (W)	Q (W)	Q (W)	Q (W)	Q (W)	Q (W)	Q (W)	Q (W)	Q (W)	Q (W)	Q (W)
5	1074.14	1194.35	1245.11	1330.36	1211.71	1348.81	1416.69	11.191	15.9171	23.8535	12.8071	25.5706	31.8905
5.5	1105.36	1256.69	1312.59	1406.42	1295.63	1445.67	1520.38	13.6906	18.7474	27.2358	17.213	30.7867	37.5455
6	1122.72	1287.90	1369.69	1451.39	1371.86	1535.61	1596.43	14.7124	21.9971	29.2737	22.1906	36.7757	42.1929
6.5	1148.75	1305.25	1416.42	1527.44	1441.17	1618.65	1662.13	13.6231	23.3009	32.965	25.4557	40.9049	44.6901
7	1164.36	1357.20	1452.77	1596.58	1503.56	1694.76	1741.64	16.5616	24.7698	37.1202	29.1311	45.5528	49.5783
(m³/s) (L/m)	Ui (W/m^2°C)	Ui (W/m^2°C)	Ui (W/m^2°C)	Ui (W/m^2°C)	Ui (W/m^2°C)	Ui (W/m^2°C)	Ui (W/m^2°C)	Ui (W/m^2°C)	Ui (W/m^2°C)	Ui (W/m^2°C)	Ui (W/m^2°C)	Ui (W/m^2°C)	Ui (W/m^2°C)
5	797.47	880.72	924.67	997.14	895.96	1012.01	1071.85	10.4398	15.9515	25.0386	12.3507	26.9033	34.4068
5.5	818.98	926.69	972.81	1055.24	959.95	1086.94	1152.72	13.1521	18.7827	28.8476	17.213	32.7184	40.7504
6	830.16	946.86	1015.13	1087.85	1016.44	1159.39	1212.94	14.0568	22.2805	31.0408	22.4381	39.6582	46.109
6.5	848.55	957.69	1050.83	1146.04	1067.79	1224.64	1265.54	12.8624	23.8377	35.0582	25.8367	44.322	49.1409
7	859.22	995.81	1077.80	1200.40	1114.01	1283.58	1326.07	15.8979	25.4392	39.7086	29.6538	49.3898	54.3348
(m³/s) (L/m)	hi (W/m^2°C)	hi (W/m^2°C)	hi (W/m^2°C)	hi (W/m^2°C)	hi (W/m^2°C)	hi (W/m^2°C)	hi (W/m^2°C)	hi (W/m^2°C)	hi (W/m^2°C)	hi (W/m^2°C)	hi (W/m^2°C)	hi (W/m^2°C)	hi (W/m^2°C)
5	2449.10	3188.90	3355.50	3457.80	3197.50	3376.10	3487.01	30.2072	37.0095	41.1868	30.5584	37.8507	42.3793
5.5	2728.56	3409.22	3587.32	3696.69	3419.89	3610.04	3728.63	24.9456	31.473	35.4812	25.3368	32.3055	36.6519
6	3004.11	3622.05	3812.73	3928.21	3635.48	3837.61	3962.91	20.5698	26.9171	30.7612	21.0169	27.7452	31.9162
6.5	3276.07	3830.73	4032.39	4155.32	3845.67	4059.48	4191.21	16.9308	23.0864	26.8387	17.3868	23.9131	27.9343
7	3547.28	4035.25	4246.86	4377.16	4050.98	4276.20	4414.96	13.7561	19.7216	23.3948	14.1997	20.5486	24.4605
(m³/s) (L/m)	Re	Re	Re	Re	Re	Re	Re	Re	Re	Re	Re	Re	Re
5	3141.74	3155.89	3163.82	3174.92	3155.57	3169.51	3177.17	0.45059	0.70272	1.05604	0.44022	0.88385	1.12785
5.5	3449.07	3466.31	3475.00	3487.18	3467.67	3482.97	3491.39	0.49976	0.75178	1.10487	0.53929	0.98294	1.22697
6	3755.19	3772.05	3785.26	3796.61	3779.15	3795.81	3803.08	0.44913	0.80069	1.10318	0.63816	1.08183	1.27524
6.5	4060.10	4080.33	4094.59	4108.91	4090.02	4108.03	4113.83	0.49811	0.84945	1.20208	0.73683	1.18051	1.32336
7	4368.11	4389.85	4403.01	4420.58	4400.27	4419.63	4425.86	0.4977	0.79881	1.20114	0.73611	1.17936	1.32211
(m³/s) (L/m)	Nu	Nu	Nu	Nu	Nu	Nu	Nu	Nu	Nu	Nu	Nu	Nu	Nu
5	19.15	24.96	26.30	27.14	24.92	26.22	27.00	30.3499	37.3424	41.7018	30.127	36.9417	41.0064
5.5	21.34	26.69	28.12	29.02	26.66	28.04	28.88	25.0754	31.7848	35.9676	24.9083	31.4179	35.3186
6	23.50	28.37	29.90	30.84	28.34	29.82	30.70	20.7022	27.2108	31.2305	20.5893	26.8736	30.6216
6.5	25.63	30.01	31.62	32.63	29.98	31.54	32.47	17.0524	23.3641	27.2793	16.9585	23.0535	26.6714
7	27.76	31.61	33.31	34.37	31.59	33.23	34.21	13.8743	19.9985	23.8235	13.783	19.7123	23.2319

5.2 Future Work

For the future work;

- It can use another sizes of the same types of the nanoparticles that used in the present experiments.
- It can use another types of nanoparticles instead of Al_2O_3 and TiO_2 nanoparticles.
- It can use another initial temperature conditions.
- It can use different values of flow rate.

Reference

[1] P. C. M. Kumar, J. Kumar, S. Sendhilnathan, R. Tamilarasan, and S. Suresh, "Heat transfer and pressure drop of Al $_2$ O $_3$ nanofluid as coolant in shell and helically coiled tube heat exchanger," vol. 46, no. 4, pp. 743–749, 2014.

[2] Y. R. Guide and P. Solutions, "The Importance of Maintaining a Generator ' s Cooling System."

[3] K. Lunsford, "Increasing heat exchanger performance," *Hydrocarb. Eng.*, pp. 1–13, 1998.

[4] J. Vlachopoulos and D. Strutt, "Asic Heat Transfer and Some Applications in Polymer Processing," *Plast. Tech. Toolbox*, vol. 2, pp. 21–33, 2002.

[5] K. Anand, V. K. Pravin, and P. H. Veena, "Enhancement of Heat Transfer Rate in Shell and Tube Heat Exchanger With Helical Tapes," *Int. J. Res.*, vol. 1, no. 10, pp. 400–406, 2014.

[6] G. Tsegay, "Design of shell and tube heat exchanger," vol. 4, no. i, p. 46, 2013.

[7] A. Barde, "AN OVERVIEW OF SHELL AND TUBE HEAT EXCHANGER PERFORMANCE," vol. 4, no. 2, pp. 58–66, 2016.

[8] S. Sunku and V. Reddy, "Enhancement of Heat Transfer in Shell and Tube Heat Exchanger Using MGO Nano Fluid," *Int. J. Res. Appl. Sci. Eng. Technol.*, vol. 3, no. 9, pp. 150–158, 2015.

[9] J. Albadr, S. Tayal, and M. Alasadi, "Heat transfer through heat exchanger using Al2O3 nanofluid at different concentrations," *Case Stud. Therm. Eng.*, vol. 1, no. 1, pp. 38–44, 2013.

[10] R. D. Arvind *et al.*, "Heat Transfer Analysis Of Shell And Tube Heat

Exchanger Using Aluminium Nitride - Water Nanofluid," vol. 1, no. 1, pp. 13–15, 2015.

[11] C. Cheng, "Experimental Investigation of Heat transfer rate of Nano fluids using a Shell and Tube Heat exchanger."

[12] M. Engineering, "Experimental Studies on Heat Transfer of Alumina / Water Nanofluid in a Shell and Tube Heat Exchanger With Wire Coil Insert," vol. 7, no. 1, pp. 16–23, 2012.

[13] K. K. Khan and G. P. K. Yadav, "Experimental Investigation of Helical Baffles Shell and Tube Heat Exchanger Using Aluminium OXIDE (II) Nanoparticle," no. 11, pp. 527–531, 2016.

[14] A. J. N. Khalifa and M. a. Banwan, "Effect of Volume Fraction of γ-Al 2 O 3 Nanofluid on Heat Transfer Enhancement in a Concentric Tube Heat Exchanger," *Heat Transf. Eng.*, vol. 11, no. January, pp. 00–00, 2015.

[15] J. O. B. Stress, I. T. S. Impact, and O. N. Performance, "© I a E M E," vol. 6324, pp. 19–27, 2014.

[16] A. K. Tiwari and I. Introduction, "THERMAL PERFORMANCE OF SHELL AND TUBE HEAT," no. 1, pp. 27–31, 2015.

[17] R. Dharmalingam, K. K. Sivagnanaprabhu, J. Yogaraja, and R. Mohan, "Experimental Investigation of Heat Transfer Characteristics of Nanofluid Using Parallel Flow , Counter Flow and Shell and Tube Heat Exchanger," *Arch. Mech. Eng.*, vol. LXII, no. 4, pp. 509–522, 2015.

[18] R. M. Ghodke, B. M. Chaure, R. D. Ankush, and N. R. Pawar, "A REVIEW OF EXPERIMENTAL STUDIES OF HEAT TRANSFER CHARACTERISTICS OF NANO FLUIDS," vol. 4, no. 3, pp. 24–31, 2017.

[19] Z. Ling, Z. He, T. Xu, X. Fang, X. Gao, and Z. Zhang, "Experimental and Numerical Investigation on Non-Newtonian Nanofluids Flowing in Shell Side of Helical Baffled Heat Exchanger Combined with Elliptic Tubes," *Appl. Sci.*, vol. 7, no. 1, p. 48, 2017.

[20] S. Heydari, Ali .Shater, Mostafa. Sanjari, "Performance investigation of

baffled shell and tube heat exchanger using different nano-fluids," *16th Conf. Fluid Dyn.*, no. April 2016, pp. 17–19, 2015.

[21] W. Conference and A. Sciences, "Performance Investigation of a Shell and Tube Heat Exchanger Using Water Based Al $_2$ O $_3$ as a Nanofluid," no. October, pp. 53–56, 2015.

[22] R. Irwansyah, J. Massing, C. Cierpka, and C. J. K??hler, "Investigation of the heat transfer in a square microchannel with Al_2O_3-H_2O nanofluids," *Tech. Mess.*, vol. 82, no. 11, pp. 572–577, 2015.

[23] F. A. Saleh, L. J. Habeeb, and B. M. Maajel, "Investigations of Heat Transfer Augmentation for Turbulent Nanofluids Flow in a Circular Tube : Recent Literature Review," vol. 1, no. 4, pp. 60–65, 2015.

[24] a. S. Dalkilic *et al.*, "Forced Convective Heat Transfer of Nanofluids - A Review of the Recent Literature," *Curr. Nanosci.*, vol. 8, no. 6, pp. 949–969, 2012.

[25] J. Holman, "Heat Transfer," *Mc Graw Hill*, p. 758, 2010.

[26] M. AL-SAMMARRAIE, "HEAT TRANSFER PERFORMACE OF DOUBLE PIPE HEAT EXCHANGER USING Al_2O_3/WATER AND TiO_2/WATER NANOFLUIDS," ANKARA, 2017.

[27] J. D. Brown, "Standard error vs Standard error of measurement," *Shiken JALT Test. Eval. SIG Newsl.*, vol. 3, no. 1, pp. 20–25, 1999.

[28] B. Harding, C. Tremblay, and D. Cousineau, "Standard errors: A review and evaluation of standard error estimators using Monte Carlo simulations," *Quant. Methods Psychol.*, vol. 10, no. 2, pp. 107–123, 2014.